SOLAR NEBULA CHEMISTRY: ORIGIN OF PLANETARY, SATELLITE, AND COMETARY VOLATILES

R. G. PRINN and B. FEGLEY, JR.
Massachusetts Institute of Technology

Complex interactions between chemical, physical and dynamical processes in the solar nebula are hypothesized to have played seminal roles in determining the reservoirs of volatile compounds and elements in the planets and their satellites and in comets. These processes include condensation, homogeneous and heterogeneous thermochemical and photochemical reactions, and disequilibration resulting from fluid transport, condensation, and cooling whenever they occur on time scales shorter than those for the chemical reactions. The ultimate potential starting materials were gases and grains in the pre-nebula interstellar cloud(s). As the nebula was forming the grains may have partially or completely evaporated or decomposed but not necessarily so. Extensive evidence from meteorites and inferences that asteroids are meteorite parent bodies implies that the nebula was extensively physically mixed and chemically reprocessed (but not necessarily chemically and isotopically homogenized) at least out to 4 AU. Possible energy sources for driving nebula chemical reactions include shock waves and photons from lightning discharges, radioactive decay processes, and solar and stellar photons, but we show that all of these are secondary to the thermal energy of the solar nebula itself. The enormous ultraviolet opacity of the gaseous nebula disk (due to H_2O, grains, etc.) caused solar ultraviolet photons to be absorbed only in the very hot inner nebula where rapid thermochemical reactions probably prevented significant photochemical disequilibration beyond some possible subtle effects on high temperature refractory material. Also, the high dust opacity in the immediate post-nebula solar system probably prevented the high ultraviolet flux from the early Sun being an effective energy input into early planetary atmospheres. Ultraviolet emission from the early Sun would still be remotely observable since the opacity for all photons emitted in directions other than toward the gaseous or dusty disk was probably very small. Surface catalysis was undoubtedly important in the nebula for (thermochemical)

In *Origin and Evolution of Planetary and Satellite Atmospheres* (1989), S. Atreya, J. Pollack, and M. S. Matthews Eds. University of Arizona Press, Tucson.

organic synthesis. We discuss models for the chemical composition of the gases and grains as functions of space and time in the nebula and the implications of these models for the volatile contents of accreting planets, satellites and comets. The models include the pressure/temperature conditions appropriate to subnebulae around giant planets as well as those appropriate to the solar nebula itself. It is highly probable that as proposed by Lewis and Prinn the major gaseous C and N compounds in the solar nebula were CO and N_2 and that carbonaceous compounds formed from CO by Fischer-Tropsch-type reactions were present in amounts comparable to CO in order to explain recent outer solar system planetary and satellite observations. Vapor-phase hydration of silicates, like the chemical reduction of CO and N_2, was kinetically inhibited in the nebula. Formation of giant planetary satellites in well-mixed subnebulae created by spin-off *as proposed by Pollack and Bodenheimer or by a massive impact as suggested by Cameron provides a natural explanation for the occurrence of CH_4-*rich *satellites like Titan and Triton using the chemistry described by Prinn and Fegley; satellite formation in planetary accretion disks which include nonlinear effects can also explain Titan but accretion-disk-products may be reprocessed in a later-forming* spin-off *or* impact-generated *subnebula. Certain volatile ratios (e.g., CO/CH_4, N_2/NH_3, H_20 ice/silicate) in ice-rich bodies are diagnostic of their origin. For example, the observation of CH_4 and NH_3 in Halley implies that at least some of the material in this comet is neither of solar nebula nor interstellar origin but is material condensed in a subnebula of one of the giant planets.*

I. INTRODUCTION

A chemist investigating for the first time the distribution of the very volatile atmosphere-forming elements (H, O, C, N, Cl, S etc; He, Ne, Ar, etc.) and their compounds in the solar system would immediately ask why planets, satellites, comets and meteorites were endowed apparently with such different mixtures of these very volatile materials. Despite their often overemphasized similarities, the volatile element contents of the terrestrial planets Venus, Earth and Mars are significantly different and many of the differences are not attributable simply to (presently recognized) evolutionary processes; the other terrestrial planet Mercury is by comparison almost completely void of volatiles. The gaseous giant planets are all rich in H and He. But the heavier elements (O, C, N, Si, etc.) comprise only a small fraction of the masses of Jupiter and Saturn while they are a large fraction of Uranus and Neptune; and all four planets are enriched in these heavier elements relative to the Sun. The ice-rich satellites of the outer planets differ in uncompressed density (and thus implied ice/rock ratios) and, except for Titan and perhaps Triton, their atmospheres are thin and/or evanescent (e.g. Io) or essentially absent. Where data is available, comets (e.g., Halley) are more rich in CO than CH_4 whereas the converse appears to be true for ice-rich satellites (e.g., Titan, perhaps Triton?). Complex carbonaceous materials are major reservoirs of C, N, and H in carbonaceous chondrites and (by inference from reflection spectra) in many dark asteroids and some outer planetary satellites (e.g., small satellites of Jupiter and Uranus).

These intriguing patterns for volatile distribution are a result of a complex and as yet poorly understood sequence of events which began with the formation of solar system bodies in the primitive solar nebula and was followed by a wide range of both general and specific evolutionary processes on each body (see, e.g., Prinn 1982 for a review). The development of theories concerning the origin of the solar system, and more specifically the advancement of our ideas concerning the chemistry of the volatile elements in the gaseous and dusty solar nebula in which the planets formed, has been guided in large part by observations of the volatile contents of planets, planetary satellites, meteorites and comets. We will emphasize in this Chapter the origin of the volatile compounds formed from the abundant chemically reactive elements H, O, C, and N; the noble gases are discussed in the Chapter by Pepin. By way of an introduction to the chemical theories which we will address in this Chapter, we will first present here a review of some salient facts about chemically active volatiles in solar system objects observed to date.

A. Volatiles in Terrestrial Planets and Chondritic Meteorites

The observed inventories of the important volatiles expressed as CO_2, H_2O and N_2 on the three terrestrial planets which possess atmospheres and in the chondritic meteorites are summarized in Table I. No indigenous volatiles have been observed in Mercury's atmosphere at a pressure greater than 10^{-13} bar or on its surface (Lewis and Prinn 1984). The abundances in Table I illustrate that both the chondrites and Venus, Earth and Mars are depleted in C, N, and H_2O relative to solar abundances. Even the volatile-rich CI1 carbonaceous chondrites have retained only $\sim$ 5 to 10% of the solar abundances of C, N, and H_2O. The similar CO_2 and N_2 depletions for Earth and Venus indicate similar inventories of these volatiles on the two planets. Furthermore, on an absolute (g/g = gram/gram) basis, there is approximately 10 times more carbon than nitrogen on both Earth and Venus. However, Venus is apparently endowed with much less H_2O than the Earth, and Mars is apparently either volatile poor, or has outgassed less efficiently than Venus and Earth, or has lost a substantial portion of its volatile content through atmospheric erosion or escape at an earlier stage of its history.

However, comparisons of the planetary and chondritic volatile inventories are complicated by several factors. The apparently larger depletions for CO_2 and N_2 on the terrestrial planets relative to the chondritic meteorites may simply reflect partitioning of a significant fraction of their C and N inventories into iron cores and/or their silicate interiors. Similarly, the observed presence of CO_2(solid) in the Martian polar caps, and the suspected presence of subsurface water ice on Mars and of $CaCO_3$ on Venus means that the atmospheric inventories of these volatiles are likely to be underestimates of the planetary inventories (e.g., see Carr 1987; Prinn and Fegley 1987*a*).

The chondritic meteorites contain a variety of volatile-bearing phases whose occurrence and abundance vary from class to class. Carbon occurs as

TABLE I

Depletions of Important Volatiles in the Chondritic Meteorites and in Venus, Earth and Mars Relative to Solar Abundances [(g/g Si)/(g/g Si)][a]

Volatile	Venus[b]	Earth	Mars[c]	Chondritic Meteorites[d]		
				C	(H, L, LL)	E
CO_2	3×10^{-5}	3×10^{-5}	2×10^{-8}	$(0.8 - 6) \times 10^{-2}$	1×10^{-3}	$(4 - 5) \times 10^{-3}$
H_2O	2×10^{-9}	2×10^{-4}	4×10^{-12}	$(0.07 - 10) \times 10^{-2}$	$(0.2 - 2) \times 10^{-3}$	$(0.4 - 2) \times 10^{-3}$
N_2	1×10^{-5}	2×10^{-5}	5×10^{-9}	$(0.1 - 5) \times 10^{-2}$	$(4 - 6) \times 10^{-4}$	$(0.1 - 1) \times 10^{-2}$

[a]Solar abundances from Cameron (1982). The solar abundances of C, N and O (minus 15% of O assumed to be incorporated into rock as MgO + SiO_2) were expressed as CO_2/Si, N_2/Si, and H_2O/Si mass ratios for this normalization. Atmospheric inventories only were considered for Venus and Mars but atmospheric plus oceanic plus crustal inventories were considered for Earth. The abundance data for Venus, Earth and Mars are from Prinn and Fegley (1987*a* and references therein).

[b]Bulk composition models *V2*, *E5*, and *Ma2* from the *Basaltic Volcanism Study Project* (1981*b*, p. 641) were used to determine Si contents for Venus, Earth and Mars, respectively. The Si contents for the chondritic meteorite classes are from Mason (1979).

[c]Present-day atmospheric inventories of CO_2, H_2O, and N_2 on Mars.

[d]The tabulated values are for CI1, CM2, C3 carbonaceous chondrites, EH4, EH5, EL6 enstatite chondrites, and H, L, LL ordinary chondrites. Carbon data: median values from Mason (1979). Nitrogen data: median values from Mason (1979) for the C and H, L, LL chondrites. Data of Grady et al. (1986) for the E chondrites (~100 to ~1000 *ppm* N by weight). Mason (1979) gives a median value of 260 ppm N for E chondrites corresponding to a depletion factor of 3×10^{-3}. Water data: Mason (1971, 1979), Kolodny et al. (1980), Robert and Epstein (1982) and Yang and Epstein (1983) for the CI1, CM2, and C3 chondrites; Yang and Epstein (1983), McNaughton et al. (1981) and Robert et al. (1979) for H, L, LL chondrites; Boato (1954) and Yang and Epstein (1983) for the two EH4 chondrites Indarch and Abee, respectively. The range of water contents (wt. %) and the corresponding depletion factors for the carbonaceous chondrites are: CI1 chondrites, 3 – 10%, $(0.3 - 1) \times 10^{-1}$; CM2 chondrites, 1 – 16%, $(0.8 - 12) \times 10^{-2}$; and C3 chondrites, 0.1 – 2%, $(0.7 - 10) \times 10^{-3}$. If the higher values reported by Wiik (cited in Mason 1971) for the water contents of the CI1 chondrites are included, the upper limit is ~20 % (wt.) corresponding to a depletion factor of $\sim 2 \times 10^{-1}$. However, some of this water is probably terrestrial contamination (see Boato 1954).

graphite, carbides, dissolved C in Fe,Ni alloy, in diamonds, in silicon carbide, disequilibrium organic matter, and carbonates (Mason 1971; Lewis et al. 1987; Bernatowicz et al. 1987). Nitrogen occurs as dissolved N in Fe,Ni alloy, disequilibrium organic matter, nitrides, and possibly as NH_4^+ salts (Mason 1971; Kung and Clayton 1978). However, the major N-carrier(s) in the ordinary chondrites is not well characterized. Finally, hydrogen occurs as water (adsorbed, hydrated in salts and in hydrous silicates) and as organic compounds. Water contents in carbonaceous chondrites may reach 10 wt. % (see Table I; Mason 1971) but are much lower ($\sim$ 100 to 1000 ppm by weight) in the ordinary and enstatite chondrites (Robert et al. 1979,1987*a,b;* McNaughton et al. 1981; Boato 1954; Yang and Epstein 1983). The hydrogen-bearing phases in these meteorites are apparently a combination of organic matter and trace hydrous phases (e.g., see Yang and Epstein 1983; Nagahara and El Goresy 1984). The stable isotope compositions of H, C, N and O in the chondritic meteorites have recently been reviewed by Pillinger (1984); some implications of the observed D/H ratios will be discussed later.

B. Volatiles in Ice-rich Satellites and Comets

With the exception of Io and Europa, all of the satellites of the outer planets for which we have reliable estimates of mass and radius appear to have low enough densities to conclude that ice must comprise a significant fraction of these satellites. Specifically, the densities of these *ice-rich* satellites range from ≈ 1.9 g cm^{-3} for Ganymede, Callisto and Titan down to ≈ 1.2 g cm^{-3} for Mimas, Iapetus and Enceladus (see Burns 1986 for a review). Models for Ganymede, Callisto and Titan suggest that they are 27 to 57, 34 to 58 and 30 to 58% ice, respectively; models for Mimas and Dione suggest they are 45 to 54% ice, and models for Enceladus, Tethys and Iapetus suggest in contrast a 65 to 78% ice composition with the remainder again being rock in each satellite (see Schubert et al. 1986 for a review). For the Uranian satellites and for the Saturnian satellite Rhea, Johnson et al. (1987) have constructed a range of models which imply that Titania is 35 to 53% ice, Oberon 40 to 58% ice and Rhea 53 to 73% ice, with the remainder again being rock in each satellite. We do not know the densities of the Neptunian satellites (Triton, Nereid) or of Pluto and its satellite Charon with sufficient accuracy to deduce useful ice/rock ratios.

In addition to the presence of ice implied from their densities, water ice has been identified spectroscopically on the surfaces of many satellites (Ganymede, Callisto, Rhea, Iapetus, Dione, Tethys, Enceladus, Mimas, Hyperion, Saturn's rings, Titania, Oberon, Umbriel, Ariel, Miranda, Charon), methane ice has been identified on the surfaces of Triton and Pluto, N_2 and CH_4 gas dominate the atmosphere of Titan, and liquid N_2 has been tentatively identified on the surface of Triton (see Burns 1986*b*; Cruikshank and Apt 1984; Cruikshank et al. 1984; Marcialis et al. 1987). In addition, there are many of the smaller satellites whose densities are not known but whose low

albedos and reflection spectra imply the possible presence of dark carbonaceous material on their surfaces; e.g., Himalia, Elara, Pasiphae, Carme, Sinope, Lysithea, Ananke, Leda, Phoebe, and the rings of Uranus; also Iapetus has a spatially variable albedo suggesting a part water ice and part carbonaceous surface (see Cruikshank 1986).

Earth-based observations of cometary comae have led to identification of a large number of volatile species emanating from comets. Carbon, nitrogen, oxygen, sulfur and hydrogen are seen in molecules (CO, HCN, CH_3CN, H_2O), atoms (C, H, O, S), free radicals (CH, CN, CS, NH, NH_2, OH) and ions (C^+, CO^+, CO_2^+, CH^+, H_2O^+, N_2^+, OH^+, CN^+). The number abundances of H, C, N, O, S, Mg, and Fe (relative to Si = 1.0) in recent bright comets are 24.3, 3.73, 1.51, 22.3, 0.55, 1.06 and 0.9, respectively (Delsemme 1982). Except for H (which is depleted by a factor of $\approx 10^3$), these number abundances are not much different from the solar composition values particularly allowing for the factor-of-two uncertainties that accompany some of the cometary values.

Preliminary results from the Giotto mission to Halley suggest nuclear emanation rates for the gases CO, N_2, CH_4 and NH_3 relative to H_2O of 0.05 to 0.2, < 0.01 to 0.1, 0.02 and 0.01 to 0.02, respectively (Balsiger et al. 1986; Eberhardt et al. 1986; Allen et al. 1987). Thus $CH_4/CO \approx 0.1$ to 0.4 and $NH_3/N_2 > 0.1$. These abundance estimates for CH_4 and NH_3 are tentative (Allen et al. 1987) but even if they are 2 or 3 times less than estimated, their presence in comets has considerable cosmogonic implications which we will address later. The dust from comet Halley apparently consists of a predominantly *chondritic* core with an *organic* mantle composed mainly of highly unsaturated compounds (Kissel and Krueger 1987).

C. Volatiles in Giant Gaseous Planets

The four giant gaseous planets (Jupiter, Saturn, Uranus and Neptune) range in size from $\sim$ 4 to 10 times the size of the Earth with masses that are $\sim$ 15 to 300 times the Earth's mass ($M_\oplus$). These planets are composed of variable proportions of solar gas and heavy (atomic number > 2) elements, with the former fraction being H_2- and He- dominated and the latter fraction being made up of *icy* (e.g., H_2O, CH_4, NH_3) and *rocky* (e.g., MgO, SiO_2, Fe, etc.) material. The observed radii and mean densities of the four planets show that the gas/(ice + rock) ratio decreases monotonically from Jupiter ($R \sim 6.98 \times 10^4$ km,$\rho \sim 1.33$ g cm^{-3}), which is gas rich, to Neptune ($R \sim 2.45 \times 10^4$ km,$\rho \sim 1.67$ g cm^{-3}), which is (ice + rock) rich.

More detailed information about the bulk compositions of these four planets, and about the radial distribution of the gaseous and solid components, can be obtained by constructing interior structure models having several compositional zones and by fitting these models to the observed mass, radius and observed J_2 and J_4 gravitational moments. These modeling efforts which have been recently reviewed by Stevenson (1982), yield several important facts.

First, the estimated mass fractions of ice + rock for Jupiter, Saturn, Uranus and Neptune are $\sim 0.05 - 0.09$, $\sim 0.17 - 0.24$, $\sim 0.75 - 0.91$ and $\sim 0.81 - 0.96$, respectively (Pollack 1985). Second, although the *relative* proportion of ice + rock increases from Jupiter to Neptune, the *absolute* abundance of this material is approximately constant (within a factor of 2) while the *absolute* abundance of the solar gas component varies by about a factor of 100. Third, the ice/rock mass ratios for Uranus and Neptune are > 1 (Hubbard 1984*a*, and references therein). More details of interior modeling efforts are described in the chapter by Hubbard.

Although the solar gas component is H_2 and He dominated, remote sensing observations show that the relative proportions of H_2 to He and of several less abundant gases (e.g., CH_4, NH_3) to H_2 also vary from planet to planet (Gautier and Owen 1985). In particular, the H_2/He ratio is approximately solar (within the large observational uncertainties) on Uranus, is slightly enhanced over solar on Jupiter, and is enhanced by a factor of ~ 2 (or more) on Saturn (Conrath et al. 1987; Hanel et al. 1986; Gautier and Owen 1985). No accurate data are available for the H_2/He ratio on Neptune. The significantly increased H_2/He ratio on Saturn and the slightly increased H_2/He ratio on Jupiter if real are plausibly explained by an inhomogeneity in the radial distribution of He rather than by the segregation of He from H_2 in the region of the solar nebula where Saturn formed. Also, the CH_4/H_2 ratio for Jupiter and Saturn is slightly enhanced over the solar composition value by ~ 2 to 5 times while much larger enhancements of ~ 20 to 25 times are observed on Uranus and Neptune. Other hydrides (e.g., NH_3, H_2O, H_2S, etc.) are expected to exhibit similar behavior, but the observations of (or attempts to detect) these gases are complicated by condensation processes, photochemical destruction and vertical mixing in these planetary atmospheres. These topics are discussed at length in several other chapters (see those of Gautier and Owen, Pollack and Bodenheimer, and Hubbard).

II. NEBULA CHEMISTRY

A. Starting Materials: Interstellar Gases and Grains

The abundant volatile elements giving rise to atmospheres must have been present in the dust and gas of the interstellar cloud(s) which collapsed to form our primitive solar nebula. Telescopic observations of dense interstellar clouds indicate the presence of a rich assortment of carbon-, oxygen- and nitrogen-containing compounds in addition to molecular hydrogen which is the probable principal constituent. Knowledge of the dust in these clouds is less definitive but there is tentative evidence that silicates, magnetite, carbonaceous compounds including graphite and ices are all present. The dust thus bears some similarity to the *primitive* material in our present solar system (e.g., carbonaceous chondrites). A detailed review of interstellar clouds is given in the chapter by Irvine and Knacke.

The bulk elemental composition of the specific cloud(s) which collapsed to form our own solar system is inferred largely from data on the composition of the Sun for the volatile elements and of CI1 carbonaceous chondrites for the less volatile ones. A summary of the abundances of the most common elements in the solar system is given in Table II (Cameron 1982).

The collapse of the precursor interstellar cloud into a rotating disk-shaped primitive solar nebula was accompanied by increasing temperatures and densities within the nebula. A central question concerns the extent to which the interstellar dust and gas metamorphosed as it was accreted by the nebula and flowed inward toward the Sun. Extensive evaporation and re-equilibration of the interstellar material is possible to the extent that the material can be transported inwards to sufficiently warm temperatures, chemically reprocessed, and then either accreted locally or transported outwards again. The meteoritic evidence discussed by Niederer and Papanastassiou (1984) and Grossman and Larimer (1974) suggests that extensive chemical reprocessing occurred in at least the inner solar system and we will discuss later tentative evidence for some chemically reprocessed material even in Comet Halley.

B. Thermochemistry, Shock Chemistry, Photochemistry and Radiochemistry

Chemical reprocessing of interstellar material in the solar nebula requires in general a source of energy; either to overcome activation energy barriers or to drive otherwise endothermic reactions such as dissociations. There are several readily recognized sources of energy for chemical reactions in the nebula.

Thermochemistry Using Thermal Energy from Nebular Accretion. During the nebular collapse phase and prior to the formation of an active proto-Sun the major source of energy was undoubtedly conversion of gravitational potential energy to kinetic (thermal) energy. The net energy flux (radiative and convective) through the nebula is given roughly by $\phi_T = sT_e^4$ where T_e is the *effective* temperature of the nebula and s is Stefan's constant (for illustrative T_e of 100 to 500 K, $sT_e^4 = 5.7$ to 3544 J $m^{-2}s^{-1}$). Endothermic chemical reprocessing requiring an energy flux ϕ exceeding ϕ_T would lead to catastrophic

TABLE II
Ratios Relative to H_2 of the 10 Most Abundant Elements in a Solar-Composition Medium[a]

H_2	1.0	N	1.74×10^{-4}
He	0.135	Mg	7.97×10^{-5}
O	1.38×10^{-3}	Si	7.52×10^{-5}
C	8.35×10^{-4}	Fe	6.77×10^{-5}
Ne	1.95×10^{-4}	S	3.76×10^{-5}

[a]Table after Cameron (1982).

local cooling and thus could not be sustained. The availability of thermal energy for driving *thermochemical* reactions is, however, highly temperature dependent since the conversion efficiency varies roughly as the Boltzmann factor $b = \exp(-E/kNT)$ where N is Avogadro's number, E is the activation energy for the reaction of interest, T is the local temperature, and k is Boltzmann's constant (e.g., for $E = 5 \times 10^4$ J/mole, $b = 0.13$ at 3000 K and 2×10^{-9} at 300 K). When b values for all relevant reactions are sufficiently close to unity (i.e., when temperatures are sufficiently high), then the system essentially is in thermochemical equilibrium and there is no net conversion between molecular kinetic (thermal) and molecular internal energy. As the temperature is lowered, thermochemical equilibrium can be maintained provided the system cools at a sufficiently slow rate. Specifically, we need the chemical reaction time $t_{chem} = -(d\ln C/dt)^{-1}$ to be $\leq$ the cooling time $t_{cool} = -(d\ln T/dt)^{-1}$ where C is concentration. Once $t_{chem} > t_{cool}$, the reaction is quenched essentially and thermochemical equilibrium no longer applies. Since for a reaction with rate $R \propto \exp(-E/kNT)$ the chemical deceleration time in a cooling system $t_{decel} = -(d\ln R/dt)^{-1} = (kNT/E)t_{cool} << t_{cool}$, then almost all cooling systems will ultimately reach disequilibrium states as $T \rightarrow 0$. For later discussion, we will assume that the usable thermal energy flux for endothermic thermochemical reactions $\phi \approx b\phi_T$; for thermo-neutral (equilibrium) and exothermic reactions there are of course no net external energy sources required but the activation energy barrier must still be overcome so the same formula can be justified.

Chemistry in Lightning Discharges and Thundershocks. The simultaneous presence of fluid motions and abundant particles in the solar nebula make charge separation (and hence lightning discharges and their accompanying thundershocks) a likely but at the present time speculative phenomenon. In effect, such discharges convert a (very small) fraction ϵ of the convective energy flux into intense electric currents, shock waves and ultraviolet photons all of which are then convertable with high efficiency into chemical potential energy through the breaking of chemical bonds. For Earth and Jupiter the lightning energy flux ϕ is approximately 4×10^{-7} and 4×10^{-5}, respectively, of the net flux in moist convective regions (Borucki et al. 1984); that is $\phi = \epsilon s T_e^4$ where $\epsilon \approx 4 \times 10^{-7}$ to 4×10^{-5}. It is arguable whether similar ϵ values apply in the nebula where the convection is largely dry but, if it does apply, then $\phi = (2.3 \text{ to } 1418) \times 10^{-5}$ J m^{-2}s^{-1} for nebular $T_e = 100$ to 500 K and $\epsilon = 4 \times 10^{-6}$. The temperatures attained in lightning are several thousand Kelvin (and hence the Boltzmann factors $b \rightarrow 1$) so that the number of chemical bonds broken per unit area per unit time $\phi_B \rightarrow \phi/D$ where D is a representative bond energy. However, a good deal of subsequent recombination occurs during cooling prior to quenching so the net ϕ_B is less than ϕ/D (e.g., on the Earth the net $\phi_B \approx 0.1 \times \phi/D$ using $D = 5 \times 10^5$ J/mole appropriate to O_2).

Photochemistry Driven by the Proto-Sun: Opacity Dilemmas. In the present-day solar system, ultraviolet light from the Sun provides a potent disequilibration mechanism in planetary atmospheres. The present-day flux F of the photochemically important Lyman-α radiation at 1 AU is not large (3.5×10^{11} photon $cm^{-2}\,s^{-1}$; 5.7×10^{-3} J $m^{-2}\,s^{-1}$), but the early Sun may have emitted a flux some 10^3 to 10^4 times greater than the present Sun (see, e.g., Zahnle and Walker 1982 for a comprehensive review). It has recently been conjectured that enhanced ultraviolet radiation from the proto-Sun served as an important disequilibration mechanism for nebula gases (Yung et al. 1987*a*), and (presumably after dissipation of the nebula) as both a disequilibration process and an energy source for hydrodynamic escape in evolving protoplanetary atmospheres (Zahnle and Walker 1982). Are these latter conjectures plausible?

First, it is arguable whether the proto-Sun was a powerful source of ultraviolet radiation while the dense *gaseous* nebula was present; current theories and observations do not enable definitive conclusions. To assess the viability of protosolar-driven photochemistry in the gaseous nebula, it is additionally important to determine the *ultraviolet* opacity of the nebula itself. In particular, if the opacity is very large the protosolar photons will be absorbed wholly in the very hot ($T \geq 2500$ K) relatively dense inner nebula where large thermochemical reaction rates involving abundant thermally produced radicals and atoms overwhelm or negate the dissociative effects of the ultraviolet photons. The solar ultraviolet photons then effectively become another source of heating to be added to the dominant source (namely conversion of the kinetic energy of infalling material to thermal energy). We note parenthetically that this situation in the gaseous inner nebula would be very different from that in the present-day terrestrial thermosphere where solar ultraviolet photons are the dominant source of energy for dissociation, where molecular diffusion, gravitational stratification and selective escape are important processes, and where pressures are much lower (and recombination reactions therefore much slower).

To calculate the minimum ultraviolet opacity we will deliberately use one of the lightest mass nebula models, specifically that of Hayashi (1981). The vertical optical depth (τ_z measured from midplane to outer surface of nebula at radius $r = r_1$) and radial optical depth (τ_r measured between radii r_1 and r_2) are:

$$\tau_z(r_1) = \frac{1}{2}\left(\Sigma_{\text{gas}}\,\sigma_{\text{gas}} + \Sigma_{\text{dust}}\,\sigma_{\text{dust}}\right) \tag{1}$$

$$\tau_r(r_1, r_2) = \int_{r_1}^{r_2} \left(\rho_{\text{gas}}\,\sigma_{\text{gas}} + \rho_{\text{dust}}\,\sigma_{\text{dust}}\right) dr. \tag{2}$$

We use the Hayashi (1981) expressions for vertical column mass densities for

gas and dust (Σ_{gas}, Σ_{dust}) and midplane gas and dust mass density (ρ_{gas}, ρ_{dust}). For the Lyman-α wavelength ($\approx$ 122 nm), the minimum value of the gas absorption cross section σ_{gas} is given by considering the absorption cross section due to H_2O alone (1.59×10^{-17} cm^2 molecule^{-1}; Kley 1984). For a nebular H_2O molar mixing ratio of 10^{-3} and nebular mean molecular weight of 2.3, we thus have $\sigma_{gas} = 1.59 \times 10^{-17} \times 6 \times 10^{23} \times 10^{-3}/2.3 = 4.1 \times 10^3$ cm^2 g^{-1}. For the dust, we have $\sigma_{dust} \approx 3/(4aD)$ provided the particle radius $a >> 122$ nm. Specifically for $a = 10^{-4}$cm and particle density $D = 4.4$ g cm^{-3} (i.e., silicate plus metal), $\sigma_{dust} \approx 1.7 \times 10^3$ cm^{2}g^{-1}. Thus since $\sigma_{dust} \approx 0.4\ \sigma_{gas}$ and also $\Sigma_{dust} \approx 0.01\ \Sigma_{gas}$(Hayashi 1981), we can ignore the small additional ultraviolet opacity due to the dust (this is reasonable unless the dust has a much smaller scale height than the gas (e.g., 250 times smaller) in which case the dust and gas opacities in the central plane could be comparable). Hence we obtain:

$$\tau_z(r_1) \simeq \frac{1}{2} \times 1.7 \times 10^3 \left(\frac{r_1}{1\ \text{AU}}\right)^{-3/2} \times 4.1 \times 10^3$$

$$= 1.7 \times 10^7 (r_1 = 0.35\ \text{AU}) \tag{3}$$

$$\tau_r(r_1, r_2) \simeq 1.4 \times 10^{-9} \times 4.1 \times 10^3 \times 1.5 \times 10^{13} \times \left[\left(\frac{r_1}{1\ \text{AU}}\right)^{-7/4} - \left(\frac{r_2}{1\ \text{AU}}\right)^{-7/4}\right] / 1.75$$

$$= 2.6 \times 10^8 (r_1 = 0.35\ \text{AU}, r_2 = 1\ \text{AU}). \tag{4}$$

These massive optical depths correspond to decreases in photochemically important photon fluxes ϕ from their midplane values at 0.35 AU due to absorption alone (i.e., not even including the $1/r^2$ geometric term) by 7 million and 110 million orders of magnitude, respectively. For photons beginning at the surface of the proto-Sun (i.e., $r_1 \rightarrow 0$), the τ_z and τ_r values are several orders of magnitude greater than their values computed above at 0.35 AU (we have not presented precise values because the Hayashi (1981) ρ and Σ expressions are strictly derived only for $r_1 \geq 0.35$ AU and because H_2O begins to be thermally dissociated to OH and H for $T \geq 2500$ K). It is almost academic to add that consideration of the more massive Cameron (1978) nebula would increase these numbers by more than another factor of 10. Thus, while the gaseous nebula was present, any protosolar-driven photochemistry must have been confined to the very hot gas near the proto-Sun where its ability to induce chemical disequilibration must have been small with surviving relicts, if any, restricted to high-temperature refractory material.

After the nebula gases and fine dust were dissipated (in a T-Tauri phase), the young Sun would then be initially irradiating a vast but thin disk of orbiting objects (boulder size to planet size?). High collision rates in this disk would have provided a potent source of dust (Greenberg et al. 1978*a*) which

would not have abated until the planets as we know them today had largely accreted and collision rates had dropped dramatically: a process which probably took several 100 Myr (Safronov and Ruzmaikina 1985*a*). This is the very time during which the Sun was its most luminous in the ultraviolet (Zahnle and Walker 1982). Thus, to assess the viability of solar-ultraviolet driven photochemistry and hydrodynamic escape in early planetary atmospheres, we need to determine the ultraviolet opacity of the gas-free but very dusty, post-nebula disk. The radial optical depth τ_r can be related to the total mass $M(r)$ of dust inside radius r by

$$\tau_r = \frac{M\sigma_{\text{dust}}}{2\pi r h_{\text{dust}}} \simeq \frac{3M}{8\pi r h_{\text{dust}} aD} \tag{5}$$

where h_{dust} is the vertical scale height of the dust.

For an optical depth $\tau_r \geq 4 \ln 10 = 9.2$, a solar ultraviolet flux 10^4 times its present value will be reduced to $\leq$ present value. From Eq. (5) this is achieved provided

$$\begin{aligned} M(r) &\geq 77 \times r\, h_{\text{dust}}\, a\, D \\ &= 3.2 \times 10^{20}\ \text{g}\ (r = 1\ \text{AU}) \\ &= 5.3 \times 10^{-8}\ \text{M}_\oplus\ (r = 1\ \text{AU}) \end{aligned} \tag{6}$$

where we have used $h_{\text{dust}} \approx$ Earth radius = 6380 km, $a = 10^{-4}$ cm, $D = 4.4$ g cm^{-3}, and $r = 1.5 \times 10^{13}$ cm to obtain the numerical value. This is an extremely small value indeed. To place it in perspective, the numerical multi-body collision/accretion calculations of Greenberg et al. (1978*a*) resulted typically in about 1% of the total initial mass of colliding bodies being processed into unresolved (sub-31-m diameter) *dust* in 25,000 yr. This translates into a *dust* production rate inside 1 AU of 2.3×10^{21} g yr^{-1} or 3.8×10^{-7} $\text{M}_\oplus$ yr^{-1}. Given these massive production rates, it is difficult to argue that the $M(r)$ value required by Eq. (6) was not easily achieved while the terrestrial planets were accreting and collisions were common in the solar system. An important theoretical problem yet to be addressed is the precise duration of this dusty *high-opacity* epoch in the solar system and how the duration of this epoch compared to the duration of the enhanced ultraviolet emission from the young Sun. The latter problem is coincidentally common to Wetherill's (1981*b*) explanation for ^{36}Ar in terrestrial atmospheres.

As a postscript to this topic, it should be emphasized that the above opacity arguments refer to solar photons emitted in the direction of the (equatorial) nebula disk. Solar photons emitted in other (e.g., polar) directions may

suffer little or no absorption and escape the protosolar system. Hence the fact that ultraviolet emission is observed from T-Tauri stars is not an argument in favor of low-opacity conditions and extensive solar-driven photochemical disequilibration in the nebula disk.

Photochemistry Driven by Stellar Photons. The maximum energy flux in interstellar photons with 90 nm < wavelength < 200 nm occurs in transparent parts of our Galaxy and is about 7×10^{-7} $Jm^{-2}s^{-1}$ (see, e.g., Duley and Williams 1984). Assuming a similar flux was applicable 4.6 Gyr ago, the energy flux for driving photochemistry in the outer skin of the solar nebula disk $\phi \leq 7 \times 10^{-7}$ $Jm^{-2}s^{-1}$ with the actual value depending on the opacity of interstellar space in the vicinity of the solar nebula. The interstellar flux is thus very small but it impinges the chemically perturbable (low-temperature) parts of the nebula. Hence it does not suffer from the same solar nebula opacity dilemmas which accompany solar-driven photochemistry and it may have been larger in the past than today. Specifically, the above ϕ value corresponds to a 90 to 200 nm photon flux of $\leq 5 \times 10^{7}$ photon $cm^{-2}s^{-1}$. In the inner nebula H_2O will be a major absorber of these photons (as already noted in the previous section). At 1 AU there are about 2.2×10^{23} H_2O molecule cm^{-2} on either side of midplane in the Hayashi (1981) model so that over the 10^5 to 10^6 yr lifetime of the nebula ≤ 0.07 to 0.7% of this H_2O will be dissociated by the above photon flux. Thus the interstellar flux would have had to have been at least 10^2 to 10^3 times greater than present in order to be important in nebula chemistry. In the cold outer nebula (e.g., $T < 150$ K), the stellar ultraviolet photons will mainly be absorbed by ice/rock grains and CO gas (H_2O is essentially totally condensed and we do not expect CH_4 in the solar nebula). Thus the H_2O photochemistry discussed by Yung et al. (1987*b*) could only have proceeded in the inner nebula and would require greatly enhanced interstellar ultraviolet fluxes over present-day values. Whatever photochemistry proceeds will also need to compete with shock chemistry and with the general inward transport and thermal reprocessing of material during the solar accretion phase.

Radiochemistry Driven by ^{26}Al. The short-lived radionuclide ^{26}Al was apparently present in dust particles in the early solar nebula with an average *mass* mixing ratio f relative to H_2 + He of $\approx 2 \times 10^{-9}$ (Lee et al. 1976). Consolmagno and Jokipii (1978) have noted that the 1.83 MeV γ photons and 1.16 MeV positrons (or the 1.02 MeV γ photons produced on their annihilation by electrons) which result from ^{26}Al decay were important sources of ionization in the solar nebula. Specifically, we can show that the power produced per unit area of the nebula disk by ^{26}Al decay (i.e., the energy flux available for radiochemistry) is

$$\phi \simeq j f \Sigma_{\text{gas}}\, d/26$$
$$= 1.2 \times 10^{-9} \left(\frac{r}{1\ \text{AU}} \right)^{-3/2} \text{J m}^{-2}\,\text{s}^{-1}$$
$$= 1.2 \times 10^{-9}\ \text{J m}^{-2}\,\text{s}^{-1}\ (r = 1\ \text{AU}) \quad (7)$$

where $j = 2.97 \times 10^{-14}\ \text{s}^{-1}$ is the ^{26}Al decay rate constant, $d = 3 \times 10^{11}$ J/mole is the average available ^{26}Al decay energy, and we have again used the Hayashi (1981) expression for Σ_{gas}. Evidently ϕ for radiochemistry is very small; indeed for ionization reactions even lightning may have been a more important (albeit spatially inhomogeneous) source of energy than ^{26}Al in the nebula.

C. Synopsis

To determine what types of chemistry will dominate in the nebula it is instructive to compare the *usable* energy fluxes ϕ available for chemical reactions to the net flux $\phi_T = sT_e^4$. Specifically for representative $T = 600$ K, $r = 1$ AU, $E = 5 \times 10^4$ J/mole, $\epsilon = 4 \times 10^{-6}$ and $T_e = 300$ K we have:

$$\phi(\text{thermochemistry})/\phi_T \approx \exp(-E/kNT) = 4 \times 10^{-5} \quad (8)$$

$$\phi(\text{thunder - shock chemistry})/\phi_T \approx \epsilon = 4 \times 10^{-6} \quad (9)$$

$$\phi(\text{solar - driven photochemistry})/\phi_T \approx 10^4 \times F \exp(-\tau_r)/\phi_T \approx 0 \quad (10)$$

$$\phi(\text{stellar - driven photochemistry})/\phi_T \approx 10^{-9} \quad (11)$$

$$\phi(\text{radiochemistry})/\phi_T \approx 3 \times 10^{-12} \quad (12)$$

Clearly thermochemistry is the expected dominant chemical process at $r = 1$ AU except for reactions with very large activation energies where shock chemistry (lightning) could be comparable. Solar photons and radioactivity are totally negligible at 1 AU. Stellar photons are not important in the inner nebula ($r \leq 1$ AU) but may be quite important in the cold, outer portions of the nebula ($r \geq 10$ AU). Specifically, for a low $T_e = 100$ K the value of ϕ/ϕ_T for stellar photochemistry increases to 10^{-7} (i.e., approaching thunder-shock chemistry and much greater than thermochemistry).

As we move closer to the Sun than 1 AU, thermochemistry becomes more and more dominant (e.g., at 1500 K, ϕ (thermochemistry)/$\phi_T = 0.018$ for the E value used in Eq. (8), while lightning becomes successively more important farther from the Sun (e.g., at 150 K, ϕ (thermochemistry)/$\phi_T = 4 \times 10^{-18}$ for the same E value while ϕ (thunder-shock chemistry)/ϕ_T remains at 4×10^{-6}). As a check, we note that if we apply Eqs. (8) through (12) to the present-day Earth atmosphere ($T_e = 255$ K, $T \simeq 300$ K, and most important relatively small τ_r value), we do predict correctly that solar-driven pho-

tochemistry is the dominant (abiotic) present-day atmospheric chemical process. Note also that when these equations are applied to specific chemical reactions the E value for that specific reaction must be used.

The fact that thermochemistry appears to have been the dominant type of chemistry overall in the solar nebula places important constraints on chemical reprocessing of cold interstellar material in the nebula. In particular, the cold material will need to be transported inwards to temperatures and pressures at which reactions can proceed within the lifetime of the nebula (10^5 to 10^6 yr). These temperatures and pressures are reached by approaching the proto-Sun in the solar nebula or approaching a giant protoplanet in a protoplanetary subnebula or atmosphere. This means that a discussion of nebula chemistry can only proceed in tandem with a discussion of nebula dynamics.

III. INTERPLAY BETWEEN NEBULA CHEMISTRY, DYNAMICS AND STRUCTURE

Advances in our understanding of nebula chemistry are coupled in several important ways to advances in our knowledge of nebula dynamics and evolution. The generally accepted evolutionary picture (see, e.g., Cassen et al. 1985; chapter by Boss et al.; Morfill et al. 1985) has the original interstellar cloud collapsing inwards with material of successively higher angular momentum accreting as time progresses thus forming a growing, rapidly rotating *accretion disk*. Mass inflow through the disk into the proto-Sun then continued until the proto-Sun ignited. Extensive chemical, petrographic and isotopic evidence from meteorites and inferences that asteroids are meteorite parent bodies suggest that the solar nebular accretion disk was extensively physically mixed (but not necessarily chemically and isotopically homogenized) out to at least 4 AU from the proto-Sun (Wilkening 1977; Niederer and Papanastassiou 1984; Grossman and Larimer 1974). The giant planets accreted in the nebula perhaps with their own accretion disks but we argue here that the probable site of formation of their regular satellites was in later-forming well-mixed subnebulae *spun off* during contraction of these initially very hot planets toward their present dimensions (chapter by Pollack and Bodenheimer) or *impact-generated* subnebulae formed by a massive collision (Cameron 1975). A simplified physical picture of the nebula is shown in Fig. 1.

It seems probable that an intense T-Tauri solar wind provided an important mode for the newly ignited proto-Sun to radiate away energy and that this intense wind first blew away the thinnest part of the nebular disk (over the protosolar poles) and also decelerated the inward gas flow in the protosolar equatorial plane; ultimately this wind then swept away all the remaining unaccreted gases and fine dust in the nebula. The time span from initial cloud collapse to proto-Sun ignition and nebular blow off was about 10^5 to 10^6 yr (Cameron 1985*a*).

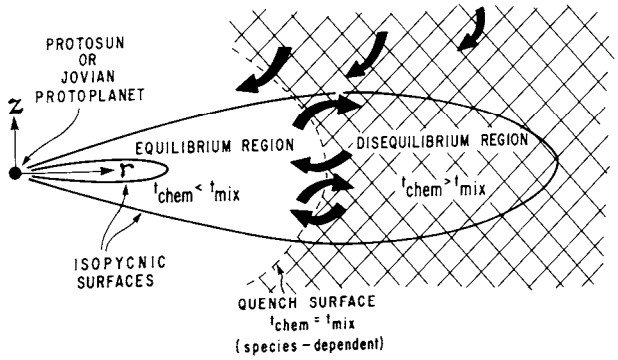

Fig. 1. Schematic illustrating the occurrence of a quench surface separating thermochemical equilibrium and transport-induced-disequilibrium regions in the solar nebula or a well-mixed protoplanetary subnebula. See text for details.

After the gaseous nebula was dissipated, the surviving bodies (ranging in size from giant gaseous protoplanets down to m-sized objects and perhaps smaller) began an evolutionary period of several 100 Myr duration characterized by high collision frequencies, accompanying accretion, fragmentation and degassing, evolution of terrestrial bodies, and further growth of the giant planets (see chapter by Greenberg). These processes proceeded in a largely gas-free but dust-rich (due to dust production in collisions) solar system environment.

Thermochemistry in both the solar nebula and protoplanetary subnebulae depended in two important ways on the pressure/temperature conditions in these nebulae. This is illustrated first in Figs. 2 and 3 where it is seen that the *P,T* profile for a representative solar nebula model (Lewis and Prinn 1980; Barshay 1981) implies that, in *thermochemical equilibrium,* CO and N_2 are much more abundant than CH_4 and NH_3 in the warm inner parts of the nebula. In contrast, CO is always less abundant than CH_4 and N_2 is at most comparable in abundance to NH_3 in the much higher-pressure (at a given *T*) protoplanetary subnebulae (Prinn and Fegley 1981). We should add that most solid/vapor and solid/solid transition temperatures in thermochemical equilibrium show much less pressure dependence than the above gas/gas transitions and thus they are much less sensitive to the choice of nebula model.

The nebula *P,T* profiles affect thermochemistry in a second important way. Because reaction rates generally increase rapidly with temperature and because the presence and abundance of efficient solid catalysts (e.g., Fe, Fe_xC particles) is temperature dependent, then the rates of the $CO \rightarrow CH_4$ and $N_2 \rightarrow NH_3$ reactions at the CO/CH_4 and N_2/NH_3 boundaries are much greater in the planetary subnebulae than in the solar nebula. As a result the $CO \rightarrow CH_4$ and $N_2 \rightarrow NH_3$ conversions are kinetically inhibited in the nebula (Lewis and Prinn 1980) but *not* in the subnebulae (Prinn and Fegley 1981*a*).

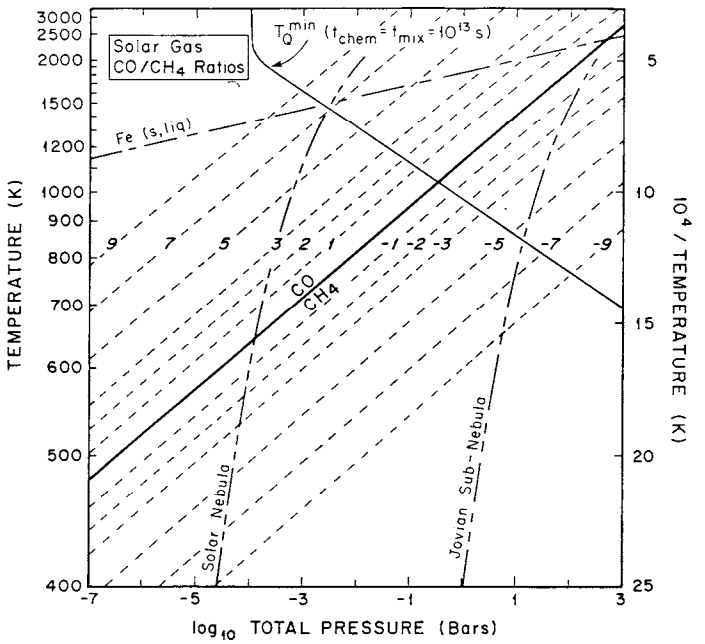

Fig. 2. Calculated ratios of CO/CH_4 at thermochemical equilibrium in a solar composition gas. The solid line labeled CO − CH_4 is the boundary where the abundances of the two gases are equal; CO is more abundant to the left and CH_4 is more abundant to the right. The dotted contours labeled 9,7,5, . . . −5,−7,−9 are constant $\log_{10} CO/CH_4$ contours. The line labeled Fe(s, liq) is the Fe condensation line; Fe(s, liq) is stable below this line. Two *P,T* profiles for an illustrative solar nebula model (Lewis and Prinn 1980; Barshay 1981) and an illustrative sub-nebula model (Prinn and Fegley 1981*a*) are also shown. The solid line labeled T_Q^{min} illustrates the minimum quench temperatures for homogeneous gas-phase conversion of CO to CH_4 assuming that the CO chemical lifetime (t_{chem}) = the maximum nebular mixing time (t_{mix}) of 10^{13} s (i.e., the nebular gases are mixed once during the nebula's lifetime). Shorter mixing times (i.e., more frequent mixing) result in higher quench temperatures. See Fig. 7 for details of Fe-catalyzed heterogeneous CO → CH_4 conversion in the solar nebula.

Thermochemistry in the nebula potentially is profoundly influenced by nebula dynamics. Current models for the solar nebula accretion disk (see, e.g., Morfill et al. 1985) indicate that outward diffusive mixing is opposed by the advective inward flow. It is therefore difficult in these models for nebula material which might have been chemically processed in the hot inner nebula to diffuse outward (Stevenson 1987*b*). This conclusion is, however, at odds apparently with the observational evidence for extensive inner nebula processing and mixing contained in chondritic meteorites (see also Cabot et al. [1987*b*] for a discussion of other problems in current models). Perhaps the solution lies in the fact that the quadratically nonlinear momentum equation is replaced by a linear diffusive momentum equation in current accretion disk

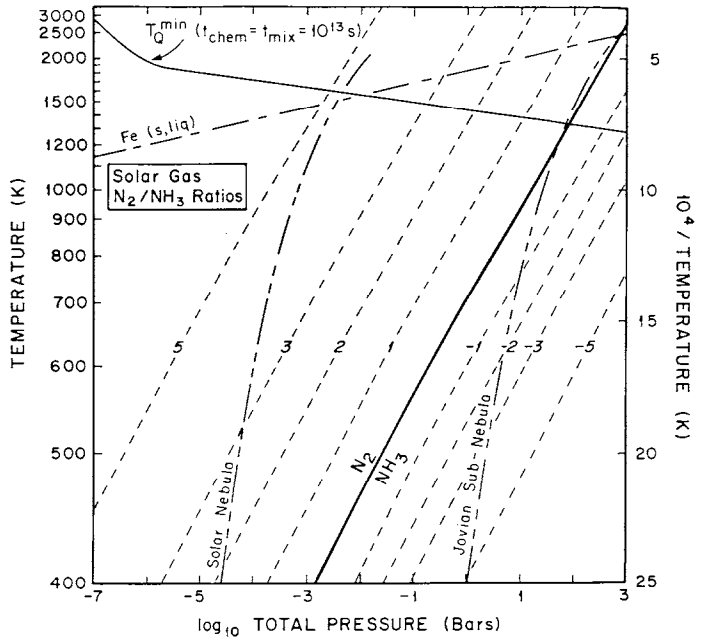

Fig. 3. As in Fig. 2 but for calculated ratios of N_2/NH_3 at thermochemical equilibrium in a solar composition gas. In this case, the line labeled T_Q^{min} illustrates the minimum quench temperatures for homogeneous gas-phase conversion of N_2 to NH_3.

models thus precluding in particular nonlinear counter-gradient momentum fluxes. These nonlinear fluxes are expected and when included in the models enable the shear to be maintained in an accretion disk in which diffusive mixing is strong enough to overcome the negative effect of the mean inward flow on outward trace constituent mixing (Prinn 1988).

Dynamics is also important in understanding the chemistry of subnebulae around the giant protoplanets. Prinn and Fegley (1981*a*) proposed a model for the chemistry in a convective circumplanetary subnebula involving inward mixing of accreted solar material (rich in CO and N_2), thermochemical conversion of the CO and N_2 to CH_4 and NH_3, and outward mixing of this processed material to form satellites rich in CH_4 and NH_3. If one assumes that the Prinn and Fegley (1981) subnebula is an accretion disk (its precise nature was in fact unspecified), then the efficiency for outward mixing in accretion disks which include nonlinear effects makes it probable that the above processed material could be mixed outward to form CH_4-rich satellites. Thus an accretion disk subnebula model may explain Titan. As mentioned earlier, it is, however, probable that the subnebulae in which outer planetary regular satellites formed were not accretion disks but later-occurring highly convective subnebulae spun off by the giant protoplanets as they contracted toward their

present dimensions (chapter by Pollack and Bodenheimer). The reprocessing of CO and N_2 to yield CH_4 and NH_3 and the formation of CH_4-rich Titan-like satellites as described by Prinn and Fegley (1981*a*) is possible in this type of subnebula model with the difference being that the inward mixing occurs during the accretion phase and the outward mixing occurs during the spin-off process.

Besides accretion disks and spin-off disks, a third type of subnebula can be formed through collision of a massive object with a planet. This has been suggested as the origin of the Moon (Cameron 1985*b*). Since collision of a large object with Uranus is hypothesized to be causal in its large obliquity, the gases blown off during this collision may have formed a subnebula in which the Uranian regular satellites condensed (Cameron 1975). The volatile element chemistry in such an *impact-generated* Uranian disk again should be qualitatively similar to that discussed by Prinn and Fegley (1981*a*). In this case, CO to CH_4 reprocessing is first accomplished in the planet itself prior to the collision with some of the reprocessing being reversed (i.e., $CH_4 \rightarrow CO$) by atmospheric shock heating due to the impact itself.

A. Chemical-Dynamical Models

The general theory for disequilibration in a thermochemical system by rapid mixing was first proposed by Prinn and Barshay (1977) to explain the occurrence of CO in the CH_4-rich Jovian atmosphere and later applied to the solar nebula and to Jovian planetary subnebulae (Lewis and Prinn 1980; Prinn and Fegley 1981*a*). In the nebula context, we first determine for each chemical species the *quench radius* (designated r_q) inside which the temperatures are high enough (and thus thermochemical reactions fast enough) to ensure that the species concentration $[i]$ is essentially equal to that in thermochemical equilibrium $[i]_e$ (general or conditional depending on the circumstances). To first order this quench radius is defined as that radius at which the chemical destruction time $t_{chem} = -[i]/(d[i]/dt)$ for the species i equals the characteristic radial mixing time t_{mix}. Since T, P and hence $1/t_{chem}$ generally decrease with altitude z, the equilibrium region bounded by the *quench surface* is convex (see Fig. 1). Outside of the quench surface or radius we must solve the continuity equation for the chemical species. The convenient coordinate system is cylindrical (r, ϕ, z) centered on the Sun or protoplanet. If mixing is sufficiently rapid relative to chemistry for parcel motions in the vertical and around a (latitude) circle, the mixing ratio f_i of a noncondensing species i at radius r is approximately independent of altitude z and azimuth ϕ. If we also model the radial trace-species flux as an eddy-diffusive flux with eddy-diffusion coefficient K, we have for the steady-state continuity equation

$$\frac{\partial^2 f_i}{\partial r^2} + \left(\frac{1}{r} + \frac{1}{\rho} \frac{\partial \rho}{\partial r} \right) \frac{\partial f_i}{\partial r} = \frac{f_i}{K t_{chem}}. \tag{13}$$

In typical nebula models the radial density gradient $d\rho/dr = -\alpha\rho/r = -\rho/H$ where H is the radial density scale length, α is a dimensionless number of order unity, and $K = l_{mix}^2/t_{mix}$ where the mixing length l_{mix} is equated in diffusive accretion disks to the vertical density scale length. It is convenient also to define a chemical length l_{chem} which is the radial length for an $e-$fold change in the destruction rate of species i. That is

$$l_{chem} = \frac{-[i]/t_{chem}}{\frac{d}{dr}([i]/t_{chem})} \tag{14}$$

where $(d\ln t_{chem}/dr)^{-1} \leq l_{chem} \leq -(d\ln\rho/dr)^{-1} = H$. For a t_{chem} with a strong temperature dependence of $\exp(A/T)$ where $A >> T$, then l_{chem} varies approximately inversely as A (i.e., inversely as the activation energy). Making the coordinate change $R = r - r_q$ and using the fact that $Kt_{chem} = Kt_{mix} = l_{mix}^2$ at $R = 0$, Eq. (13) then becomes

$$\frac{\partial^2 f_i}{\partial R^2} + \left(\frac{1-\alpha}{R + r_q}\right)\frac{\partial f_i}{\partial R} \simeq \frac{f_i(o)}{l_{mix}^2} \exp\left[-R\left(\frac{1}{l_{chem}} - \frac{1}{H}\right)\right]. \tag{15}$$

In the vicinity of the quench surface $R + r_q \simeq r_q$ and l_{chem}, H and l_{mix} can be regarded as (positive) constants. Using two appropriate boundary conditions (f_i(o) equal to its thermochemical equilibrium value $f_i(r_q, \text{equil})$ and f_i finite and positive for large R), Eq. (15) then has the simple analytical solution

$$f_i = f_i\,(r_q, \text{equil})\left(1 - \frac{l_{chem}^2}{\beta l_{mix}^2}\left\{1 - \exp\left[-\left(\frac{1}{l_{chem}} - \frac{1}{H}\right)R\right]\right\}\right) \tag{16}$$

where $\beta = (1 - l_{chem}/H)/(1 - l_{chem}/r_q)$ and the second boundary condition requires $l_{chem}^2 \leq \beta l_{mix}^2$ and $l_{chem} < H$. For $R >> l_{chem}$, the destruction of i is quenched and f_i has the constant value

$$f_i \simeq f_i(r_q, \text{equil})\left(1 - \frac{l_{chem}^2}{\beta l_{mix}^2}\right). \tag{17}$$

The interesting case occurs when $l_{chem}^2 << \beta l_{mix}^2 \simeq l_{mix}^2$ (that is, the air parcel is quenched chemically by moving a distance R much less than the mixing length) in which circumstance the mixing ratio of the species i in the diseq-uilibrium region ($r > r_q$) is constant and is given simply by its equilibrium value at the quench radius. That is

$$f_i \simeq f_i(r_q, \text{equil}) \qquad \text{for } r \geq r_q. \tag{18}$$

Clearly, the larger the activation energy for destruction of the species i, then the more likely Eq. (18) is appropriate. Note also that when Eq. (18) applies, the convex shape of the quench surface (Fig. 1) means that air parcels are quenched for vertical as well as radial motions; that is, f_i is independent of z for $r \geq r_q$ as required in Eqs. (13) through (17).

The general approach is therefore first to calculate the thermochemical equilibrium mixing ratio for the species of interest throughout the nebula. Then appropriate kinetic expressions are obtained to describe the destruction rate of i and thus t_{chem} throughout the nebula. Finally, upper and lower limits to t_{mix} are defined (e.g., a *minimum* t_{mix} might be defined by $t_{\text{mix}} = 3H/V_s$ where V_s is the sound speed and a *maximum* t_{mix} might be equated to the lifetime of the nebula). Thus a range of possible quench radii defined by t_{chem} is obtained and by comparing l^2_{chem} and l^2_{mix}, the validity of Eq. (18) is ascertained for each quench radius. The temperature at the quench radius is referred to as the *quench temperature* T_Q and it is often more convenient to define the quench position in the nebula by T_Q rather than r_q.

The reader should be aware that the above treatment does not take into account the mean inward flow of material toward the proto-Sun/protoplanet in accretion disks which we mentioned earlier. However, the aforementioned nonlinear effects allow diffusion to dominate this mean flow so the above treatment should hold approximately. This treatment is applicable without such qualifications to *spin-off* and *impact-generated* subnebulae (and for the present-day Jovian planets when cast in spherical coordinates).

B. Results of Chemical-Dynamical Models for Important C-, H-, N-, O-Bearing Volatiles

(i) Carbon and Nitrogen Compounds. The net reactions which relate CO, CH_4, CO_2, N_2 and NH_3 in a solar gas are

$$CO + 3H_2 = CH_4 + H_2O \tag{19}$$

$$N_2 + 3H_2 = 2NH_3 \tag{20}$$

$$CO + H_2O = CO_2 + H_2 \tag{21}$$

which all proceed to the right with decreasing temperature at constant pressure. However the extent to which these homogeneous gas-phase reactions approach quantitative conversions of CO to CH_4, CO to CO_2 and N_2 to NH_3 with decreasing temperature is severely limited by the rates at which the relevant rate-determining steps occur relative to the rates of nebular mixing and overall cooling.

The kinetic inhibition of reactions (19) to (21) in a solar gas can give dramatically different compositions than does the assumption of complete thermochemical equilibrium for the major carbon and nitrogen-bearing volatiles ultimately incorporated into the gases and grains accreted by planetary and cometary bodies. These differences are illustrated in Figs. 2 through 4

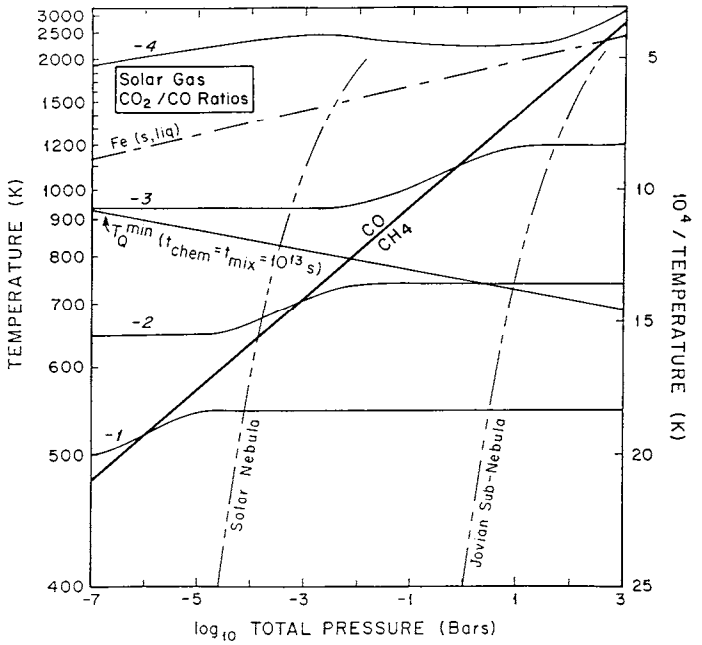

Fig. 4. As in Fig. 2 but for calculated ratios of CO_2/CO at thermochemical equilibrium in a solar composition gas. The inflections in the constant $\log_{10} CO_2/CO$ contours are caused by changes in the H_2O abundance from the CO- to CH_4- dominated regions. The T_Q^{min} line illustrates the minimum quench temperatures for homogeneous gas-phase conversion of CO to CO_2. If thermochemical equilibrium were maintained to lower temperatures and pressures, a CO_2- dominant field results (Lewis et al. 1979).

where the minimum quench temperatures for the homogeneous gas-phase conversions (Eqs. 19 to 21) are plotted along with the (CO/CH_4), (N_2/NH_3), and (CO_2/CO) ratios expected for maintenance of thermochemical equilibrium. The minimum quench temperatures, which are calculated by Prinn and Fegley (1981*a*) as described above, refer to the slowest possible nebular mixing rate of one overturn over the course of the solar nebula lifetime of $\sim 10^{13}$ s (Cameron 1985*a*; Lewis and Prinn 1980). Faster mixing rates (and thus shorter mixing times) will yield higher quench temperatures.

One very important point illustrated in Figs. 2 and 3 is that kinetic inhibition of homogeneous gas-phase $CO \rightarrow CH_4$ and $N_2 \rightarrow NH_3$ conversions almost certainly occurs at the low pressures commonly associated with solar nebula models. For the representative solar nebula model (Lewis and Prinn 1980; Barshay 1981) illustrated in Figs. 2, 3 and 4, the $CO \rightarrow CH_4$ and $N_2 \rightarrow NH_3$ conversions will quench at 1470 K and 1600 K, respectively, where $(CO/CH_4) \sim 10^7$ and $(N_2/NH_3) \sim 10^5$ (see Fig. 5). Furthermore, decreasing pressure leads to increases in these quench temperatures and to increases in the corresponding (CO/CH_4) and (N_2/NH_3) ratios at quench. Indeed at suffi-

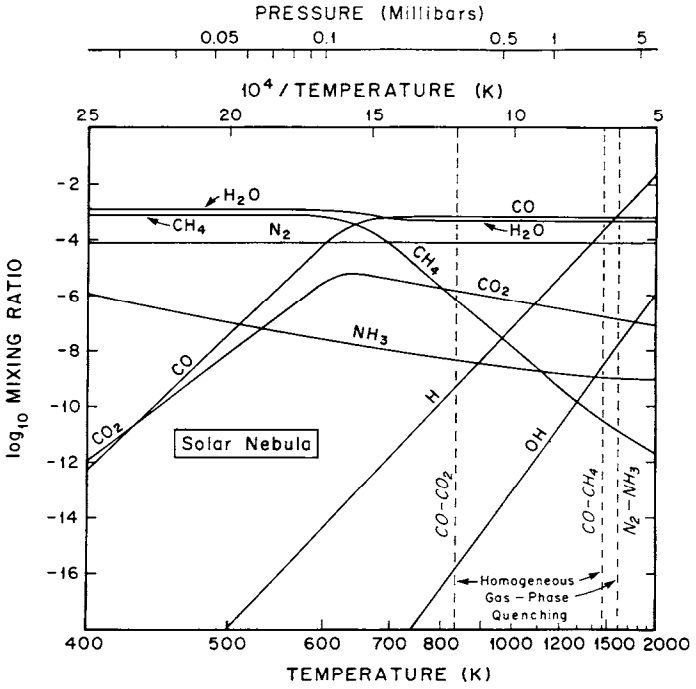

Fig. 5. Calculated equilibrium abundances of important H, C, N, O gases along the solar nebula P,T profile illustrated in Figs. 2,3 and 4. H_2 has an abundance close to 0 on a log scale and is not graphed for clarity. The vertical dashed lines illustrate the minimum quench temperatures for homogeneous gas-phase conversions of $N_2 \rightarrow NH_3$, $CO \rightarrow CH_4$, and $CO \rightarrow CO_2$ and correspond to the intersection of the T_Q^{min} lines with the solar nebula P,T profile in Figs. 2,3 and 4. The corresponding pressure scale for this model profile is also shown.

ciently low pressures of $\sim 10^{-6}$ bar, quenching will occur at such high temperatures that essentially no reprocessing of CO to CH_4 or of N_2 to NH_3 can occur even over the age of the solar system ($\sim 10^{17}$ s).

In contrast, Fig. 4 illustrates the facile nature of the homogeneous gas-phase $CO \rightarrow CO_2$ conversion, which proceeds down to $\sim$ 830 K and $(CO_2/CO) \sim 2 \times 10^{-3}$ for the representative solar nebula model shown. The relatively rapid interconversions of oxidized carbon species such as $CO\text{-}CO_2\text{-}H_2CO$ (e.g., see Warnatz 1984) strongly suggest that equilibria among these species will be maintained even at relatively low pressures ($\sim 10^{-7}$ bar). The possible dominance of CO_2 and CO_2-bearing compounds over CH_4 in low temperature nebula condensates, which was first proposed by Lewis and Prinn (1980), is a consequence of this situation.

As indicated in Figs. 2, 3 and 4, increasing pressure leads to decreasing quench temperatures for reactions (19) to (21), although this effect is not as pronounced for the $CO \rightarrow CO_2$ conversion as it is for the $CO \rightarrow CH_4$ and N_2

$\rightarrow NH_3$ conversions. The lower quench temperatures lead to smaller (CO/CH_4) and (N_2/NH_3) ratios; indeed, for sufficiently high pressures of ~ 0.3 bar for $CO \rightarrow CH_4$ and ~ 80 bar for $N_2 \rightarrow NH_3$, quenching may produce equimolar mixtures of these gases. (Although uncertainties in the kinetic data may lead to small shifts in the specific pressure values, the relative positions of the CO - CH_4 and N_2 - NH_3 boundaries in P, T space require P_{total} for $N_2 = NH_3$ to be greater than P_{total} for $CO = CH_4$.) Still higher pressures will lead to even smaller (CO/CH_4) and (N_2/NH_3) ratios. For the representative Jovian subnebula model (Prinn and Fegley 1981*a*) illustrated in Figs. 2, 3 and 4, the relevant quench temperatures and gas ratios are (CO/CH_4) $\sim 10^{-6}$ at $\sim$ 840 K and (N_2/NH_3) $\sim$ 1 at $\sim$ 1370 K (see Fig. 6). However, in contrast to the $CO \rightarrow CH_4$ and $N_2 \rightarrow NH_3$ conversions, the slightly lower quench temperatures for the $CO \rightarrow CO_2$ conversion lead to slightly larger (CO_2/CO) ratios at higher pressures. Specifically, (CO_2/CO) $\sim 10^{-2}$ at 740 K for the Jovian subnebula (*P*, *T*) profile shown. The much smaller (CO_2/CH_4) ratio in this case relative to that predicted for typical assumed solar nebula pressures of $\sim 10^{-4}$ to $\sim 10^{-7}$ bar leads to much smaller amounts of CO_2 and CO_2-bearing compounds incorporated into low-temperature condensates formed in

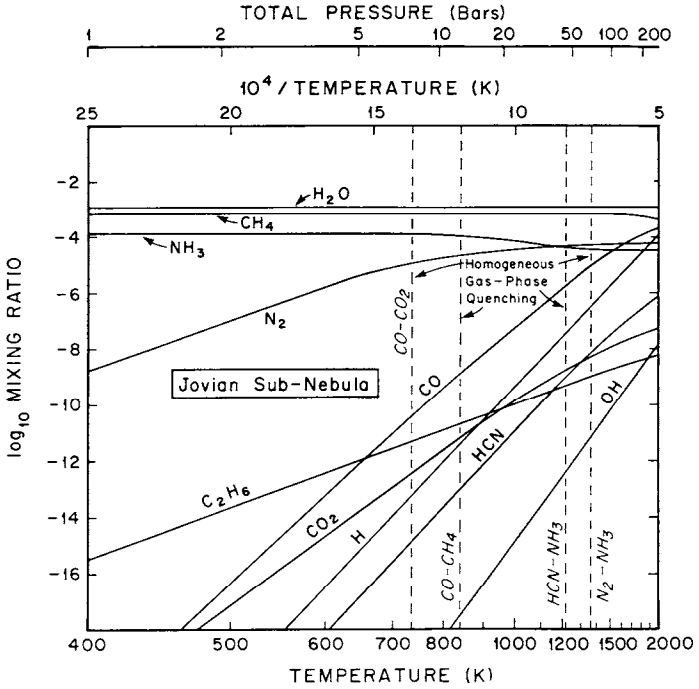

Fig. 6. As in Fig. 5 but for the Jovian subnebula *P*,*T* profile illustrated in Figs. 2,3 and 4. H_2 is not graphed for clarity.

spin off or impact-generated subnebulae around the giant planets than in solar nebula condensates (e.g., compare Prinn and Fegley 1981*a* and Lewis and Prinn 1980).

Finally, we note that small but significant amounts of HCN are predicted for homogeneous gas-phase quenching of the HCN $\rightarrow$ N_2 and HCN $\rightarrow$ NH_3 conversions over wide regions in *P, T* space covering plausible solar nebula and subnebula models. For the two representative nebular models shown in Figs. 5 and 6, quenching calculations done as described by Prinn and Fegley (1981*a*) (again assuming the slowest possible nebula mixing rate of one overturn in 10^{13} s) yield $(HCN/N_2) \sim 10^{-6}$ at $T_Q \sim 1460$ K along the solar nebula *(P, T)* profile and $(HCN/NH_3) \sim 10^{-5}$ at $T_Q \sim 1220$ K along the Jovian subnebula *(P, T)* profile. Somewhat larger amounts of HCN, which is an important precursor for the abiotic synthesis of complex organic molecules (Oro and Kimball 1961; Abelson 1966), may be produced in lightning discharges in nebular environments. This will be discussed in more detail below.

(ii) Heterogeneous Catalysis and Fischer-Tropsch-Type Reactions. The considerations discussed above for homogeneous gas-phase reactions may be modified somewhat by the presence of an abundant and active catalyst. In particular, if Fe metal grains are well mixed with the nebular (or subnebular) gases and are catalytically active, they may accelerate the rates of the CO $\rightarrow$ CH_4, $N_2 \rightarrow NH_3$ and CO $\rightarrow$ CO_2 conversions, and may also promote the synthesis of complex organic molecules from the CO and H_2 in the nebular gas via Fischer-Tropsch-type reactions. Indeed, the latter possibility was first anticipated by Urey (1953) who proposed that the CO $\rightarrow$ CH_4 conversion "may well proceed through graphite or complex tarry compounds as intermediates." The feasibility of Urey's proposal was later experimentally demonstrated by Anders and coworkers (Hayatsu and Anders 1981; Studier et al. 1968) who synthesized complex organic compounds analogous to those in carbonaceous chondrites by iron meteorite-catalyzed Fischer-Tropsch-type reactions.

The heterogeneous Fe- catalyzed $N_2 \rightarrow NH_3$ conversion may occur over temperatures between the Fe metal condensation point (e.g., see Fig. 3) and a pressure-independent temperature of $\sim$ 400 K where Fe metal is no longer stable and Fe_3O_4 forms. The incorporation of FeO into silicates may raise this latter temperature to a pressure-independent value of $\sim$ 480 K. From Figure 3 it is clear that if the heterogeneous Fe catalysis of the $N_2 \rightarrow NH_3$ conversion is effective down to $\sim$ 480 K where the last Fe metal is incorporated into FeO-bearing silicates, then for typical solar nebula pressures of $\sim 10^{-4}$ to $\sim 10^{-7}$ bar, the resulting (N_2/NH_3) ratio is much *greater* than unity. Furthermore, this conclusion is not altered if FeO-bearing silicate formation is neglected and Fe metal grains are assumed to be present (and catalytically active) in the nebular gas down to $\sim$ 400 K where they will be deactivated by formation of Fe_3O_4 coatings. However, we note that if the Fe metal grains are not well mixed with

the gas phase or are inactivated by thin coatings of FeS, which forms at a pressure-independent temperature of $\sim$ 680 K, then heterogeneous catalysis may not be effective down to such low temperatures. The results of Lewis and Prinn (1980) for the solar nebula model illustrated in Figs. 3 and 5 indicate that the minimum quench temperature for the Fe catalyzed $N_2 \rightarrow NH_3$ conversion is $\sim$ 530 K where $(N_2/NH_3) \sim 170$.

Similar arguments regarding the catalytic efficiency of Fe metal grains in higher pressure environments representative of those expected in subnebulae around the giant planets suggest that (N_2/NH_3) ratios much *less* than unity may be characteristic of these environments. Specifically for the Jovian subnebula *(P, T)* profile illustrated in Figs. 3 and 6, the results of Prinn and Fegley (1981*a*) suggest a minimum quench temperature of $\sim$ 495 K and a (N_2/NH_3) ratio of $\sim 5 \times 10^{-4}$ for the Fe-catalyzed $N_2 \rightarrow NH_3$ conversion. However, it is clear from Fig. 3 that for subnebula pressures of $\sim 10^{-2}$ to $\sim 10^2$ bar, Fe catalysis down to $\sim$ 400 K where Fe_3O_4 coatings will form will always yield (N_2/NH_3) ratios less than unity. The consideration of possible Fe catalysis of the $N_2 \rightarrow NH_3$ conversion thus does *not* alter our previous conclusions of N_2 dominance in the solar nebula and of NH_3 dominance in giant planet subnebulae that were reached on the basis of homogeneous gas-phase chemistry.

It is evident from Fig. 2 that if Fe catalysis of the $CO \rightarrow CH_4$ conversion is effective down to temperatures of $\sim$ 400 to $\sim$ 480 K, then over the entire range of pressures shown from $\sim 10^{-7}$ to $\sim 10^3$ bar, the resulting (CO/CH_4) ratios will be much *less* than unity. This contrasts with (CO/CH_4) ratios much *greater* than unity predicted for quenching of homogeneous gas-phase reactions at low pressures generally assumed for the solar nebula but reinforces conclusions regarding (CO/CH_4) ratios less than unity predicted for gas-phase quenching in subnebular environments at higher pressures.

The heterogeneous Fe-catalyzed $CO \rightarrow CH_4$ conversion in nebular and subnebular environments can be modeled using the results of laboratory studies of this reaction (e.g., see Vannice 1975,1982). The rate equation for the $CO \rightarrow CH_4$ conversion on metallic iron particles is

$$\frac{d}{dt}[CH_4] = -\frac{d}{dt}[CO] = [\text{sites}]k_{\text{site}} P_{H_2} \tag{22}$$

where $[i]$ is the number density per cm^3 of species i, P_{H_2} is the hydrogen pressure in bars and k_{site} is the experimental rate constant in units of CH_4 molecules produced per active site per s per bar on the Fe surface. The canonical value for the number of active sites per cm^2 surface is $\sim 10^{15}$. This is equivalent to a site number density of $\sim 10^5$ to 10^6 cm^{-3} in the solar nebula assuming iron present at solar abundance in the form of monodisperse, spherical (r = 100 μm) grains. A representative rate constant

$$k_{site} \sim 2.2 \times 10^7 \exp(-21{,}300/RT) \tag{23}$$

for the $CO \rightarrow CH_4$ conversion on *clean* Fe surfaces was taken from Vannice (1975). The chemical destruction time t_{chem} for the Fe-catalyzed $CO \rightarrow CH_4$ conversion is then given by

$$t_{chem} = -[CO] \Big/ \frac{d}{dt}[CO] \tag{24}$$

where the CO destruction rate is taken from Eq. (22).

Fig. 7 illustrates that the heterogeneous Fe catalysis of the $CO \rightarrow CH_4$ conversion in the solar nebula may lead to quenching of this reaction at ~ 900 K and $(CO/CH_4) \sim 10^{3.8}$ for the *minimum* radial mixing times implied by transport at 1/3 of sound speed (Cameron 1978; Lewis and Prinn 1980) or at

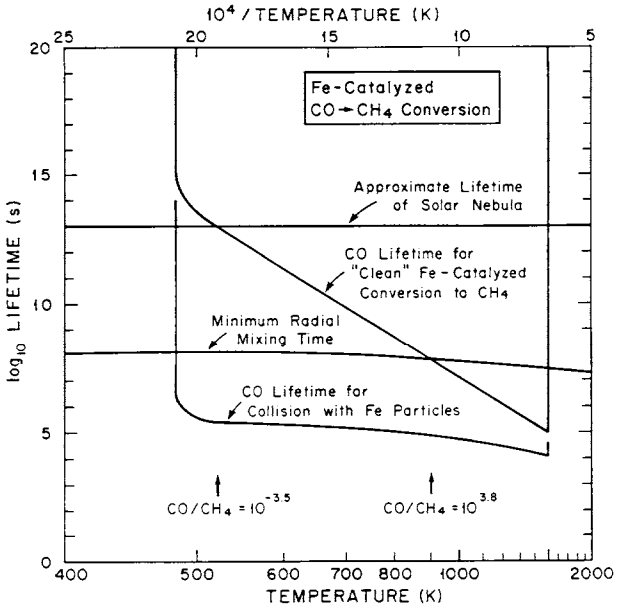

Fig. 7. Chemical and physical lifetimes associated with the Fe-catalyzed heterogeneous conversion of CO to CH_4 in the solar nebula. Fe catalysis first becomes possible at ~ 1500 K where Fe metal condenses (see Fig. 2) and becomes ineffective at ~ 480 K where the last metallic Fe is consumed by FeO incorporation into silicates. The shortest feasible nebular mixing time and the longest feasible nebular mixing time (see Sec. III.A) bracket the range of CO/CH_4 ratios produced by the heterogeneously catalyzed conversion on *clean* Fe surfaces. The expected inactivation of the Fe surface by rapidly forming carbonaceous coatings (Vannice 1982; Krebs et al. 1979), which may be similar to the "tar balls" observed in interplanetary dust particles (Bradley et al. 1984; Bradley and Brownlee 1986), will reduce the efficiency of CH_4 production.

temperatures as low as ~ 520 K and $(CO/CH_4) \sim 10^{-3.5}$ for the *maximum* radial mixing time of one overturn in 10^{13} s. However, these results, which utilize Vannice's (1975) CO destruction rate constant for clean Fe surfaces, must substantially overestimate the efficiency of Fe catalysis because the inactivation of the Fe surface by rapidly forming carbonaceous coatings (Vannice 1982; Krebs et al. 1979), which may be similar to the "tar balls" observed in interplanetary dust particles (Bradley et al. 1984; Bradley and Brownlee 1986), is not considered. Therefore, the results in Fig. 7 should be viewed as an upper limit to the efficiency of the heterogeneous Fe catalyzed $CO \rightarrow CH_4$ conversion in the solar nebula.

The more likely course of events, which is indicated by the presence of carbonaceous material in some meteorites and of tar balls in interplanetary dust particles, is the Fe-catalyzed synthesis of complex organic molecules from CO and H_2 in the nebular gas by net reactions such as

$$(2n + 1)H_2 + nCO = C_nH_{2n+2} + nH_2O \quad (25)$$

$$(n + 1)H_2 + 2nCO = C_nH_{2n+2} + nCO_2 \quad (26)$$

$$2nH_2 + nCO = C_nH_{2n} + nH_2O \quad (27)$$

$$nH_2 + 2nCO = C_nH_{2n} + nCO_2 \quad (28)$$

$$2nH_2 + nCO = C_nH_{2n+1}OH + (n - 1)\,H_2O \quad (29)$$

$$(n + 1)H_2 + (2n - 1)CO = C_nH_{2n+1}OH + (n - 1)CO_2 \quad (30)$$

which exemplify the Fischer-Tropsch synthesis of alkanes, alkenes and alcohols, respectively. Such reactions, and similar reactions forming acetylenic and aromatic compounds, will proceed spontaneously in the presence of a suitable catalyst such as Fe or Ni (Bond 1962; Biloen and Sachtler 1981).

The possible significance of Fischer-Tropsch-type reactions for the formation of organic compounds found in carbonaceous chondrites has long been recognized (see, e.g., Urey 1953; Studier et al. 1968; Hayatsu and Anders 1981). However, quantitative discussions of the amount and type of organic compounds which may have been produced by such reactions operating in possible prenebular, nebular and subnebular environments requires a detailed knowledge of the effects of process parameters (e.g., pressure, temperature, time, reactant composition, catalyst chemical and physical state, presence of catalyst poisons, etc.) on the product composition and yield. This detailed knowledge is presently unavailable (e.g., as recently pointed out by Dictor and Bell [1986], the nature of the catalytically active iron phase is still controversial) but is essential for theoretical models of carbon chemistry and organic matter production by Fischer-Tropsch-type reactions in the solar nebula.

Insight into the probable effects of these important process parameters can nevertheless be obtained by qualitative comparisons of products of

Fischer-Tropsch-type reactions run under very different sets of conditions. Figure 8 illustrates that the hydrocarbons formed at *low* total conversions of CO to products using a clean Fe surface become progressively lighter and more C_1 rich as the reactant H_2/CO ratio increases from 4 to 100 (Krebs et al. 1979). Analogous trends were observed by Vannice (1975) for CO hydrogenation over clean Fe supported on Al_2O_3 as the H_2/CO ratio increased from 0.6 to ~ 15 (note that the nebular H_2/CO ratio is ~ 1200 if all carbon is present as CO).

In contrast, hydrocarbons produced at *high* total conversions of CO to products using industrial Fe catalysts are rich in large molecules. For example, an illustrative hydrocarbon composition from a commercial reactor (Dry 1981) is C_1 (2%), C_2 (2%), C_3 (5%), C_4 (5%), C_5 to C_{11} (18%), C_{12} to C_{18} (14%), C_{19} to C_{23} (7%), C_{24} to C_{35} (21%), and $> C_{35}$ (26%). Although the details of product selectivity (e.g. alkanes vs alkenes, carbon chain length distribution, degree of branching) vary somewhat, the commercial reactors operating at high total conversion of CO to products (with recycling of the outlet gas through the reactor) generally give larger molecules than the single-pass flow experiments operating at low total conversions and large H_2/CO ratios. The static experiments of Studier et al. (1968) also gave larger maximum carbon chain lengths at lower H_2/CO ratios.

These observations suggest that the conversion of nebular CO to organic material may yield a wide range of products from CH_4 to large molecules. Environmental conditions which allow high total conversions of CO (in dynamic or static conditions) and perhaps H_2/CO ratios smaller than the solar

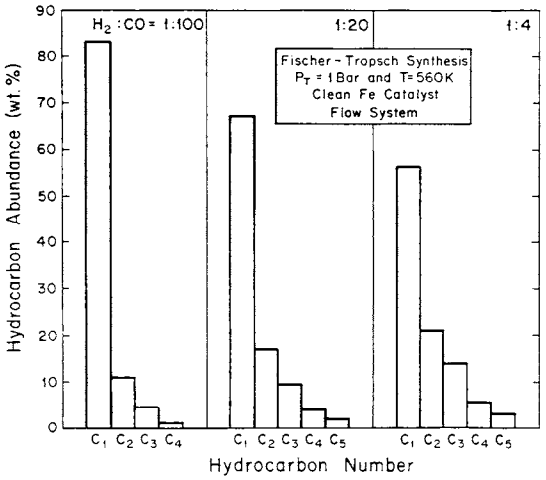

Fig. 8. Representative composition of the hydrocarbons produced by the Fischer-Tropsch synthesis on an Fe catalyst for a range of H_2/CO ratios from 1 : 100 to 1 : 4. The results are for low total conversion of CO to products in a flow system (from Krebs et al. 1979).

value of ~ 1200 may yield larger molecules than environments that allow low total conversions of CO and the solar H_2/CO ratio. In any case, the analogies between organic compounds in carbonaceous chondrites and the products of Fischer-Tropsch-type reactions (Hayatsu and Anders 1981), and the associations of carbonaceous material (tar balls) with Fe, Ni alloy, carbides and oxides (which have all been proposed as the catalytically active Fe phase [Dictor and Bell 1986]) in interplanetary dust grains (Bradley et al., 1984) suggest that Fischer-Tropsch-type reactions were operative in some environments in the solar nebula and early solar system.

(iii) Lightning and Shock Chemistry. We have mentioned earlier that lightning discharges and their accompanying thundershocks are a possible disequilibrating mechanism in nebular and subnebular environments favorable for charge separation. The high temperatures (several times 10^3 K) reached in lightning discharges lead to increasing degrees of molecular dissociation, atomization and ionization with increasing temperatures. These effects are more pronounced at lower total pressures than at higher total pressures. Recombination of these simple fragments during the rapid cooling of the shocked gas leads initially to the production of more complex fragments, then to thermally stable molecules. Sufficiently rapid cooling quenches these stable molecules at their high temperature abundances, which are generally enhanced over their equilibrium abundances at much lower temperatures (e.g., see the description by Borucki and Chameides [1984] of NO production in terrestrial lightning discharges via the shock heating and rapid quenching of $N_2 + O_2$). Repeated lightning discharges then lead to the buildup of these thermally stable species until a steady-state abundance is reached or they are lost by other processes (e.g., chemical reactions forming more complex molecules or vapor → solid condensation). Thus, lightning is a potentially significant source of disequilibrium products, especially in the cool, thermochemically inactive regions of the nebula near and beyond the water ice condensation point (T ~ 150 to 200 K over a wide pressure range).

Thermodynamic calculations of gas abundances presented in Figs. 9 and 10 and energetic considerations based on the First Law of Thermodynamics can be used to set upper limits on the production efficiencies and yields of important disequilibrium products such as HCN. Shock heating of a CO-, N_2-bearing gas parcel (e.g., in the solar nebula) produces HCN via the net reaction

$$2CO + N_2 + 3H_2 = 2HCN + 2H_2O \tag{31}$$

from which it can be easily deduced that the resultant HCN mixing ratio (X_{HCN}) is proportional to P_T the total pressure. This process is illustrated in Fig. 9 for the heating along an adiabatic (P,T) profile of an initially cool, H_2O-depleted (due to condensation) gas parcel in the outer solar nebula.

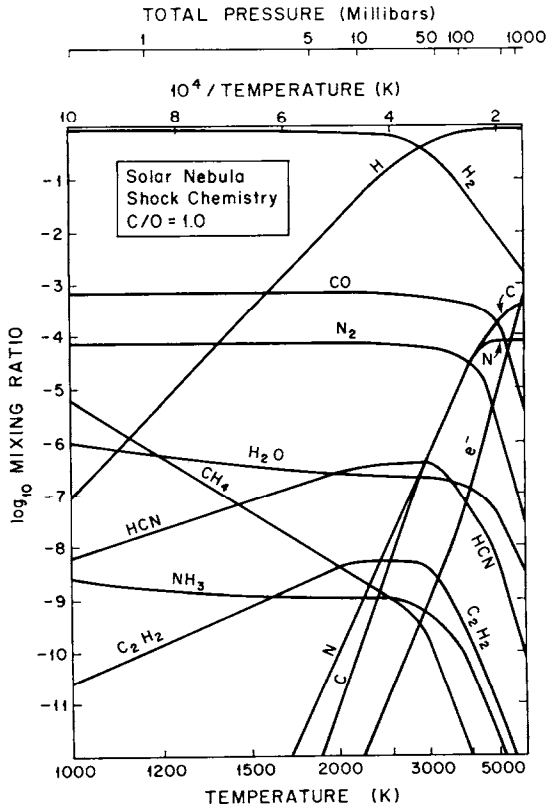

Fig. 9. Calculated equilibrium abundances of important H, C, N, O compounds in an initially cool, H_2O-depleted (by condensation) gas parcel which is shock heated by a lightning discharge in the outer region of the solar nebula. An adiabatic P,T profile is assumed; a Hugoniot or an isopycnic profile would give a lower pressure at a given temperature. The electron abundance shown is balanced by an identical abundance of positive ions (which are predominantly H^+) in order to preserve electroneutrality. However, the positive ions and many other radicals, atoms and negative ions are not graphed to simplify the figure.

On the other hand, shock heating of a CH_4-, N_2-bearing gas parcel or of a CH_4-, NH_3-bearing gas parcel (e.g., in the Jovian subnebula) produces HCN by the net reaction

$$2CH_4 + N_2 = 2HCN + 3H_2 \tag{32}$$

in the former case (where $X_{HCN} \propto P_T^{-1}$) or via

$$CH_4 + NH_3 = HCN + 3H_2 \tag{33}$$

in the latter case (where $X_{HCN} \propto P_T^{-2}$). Both of these two processes would contribute to HCN production during the heating along an adiabatic (P,T)

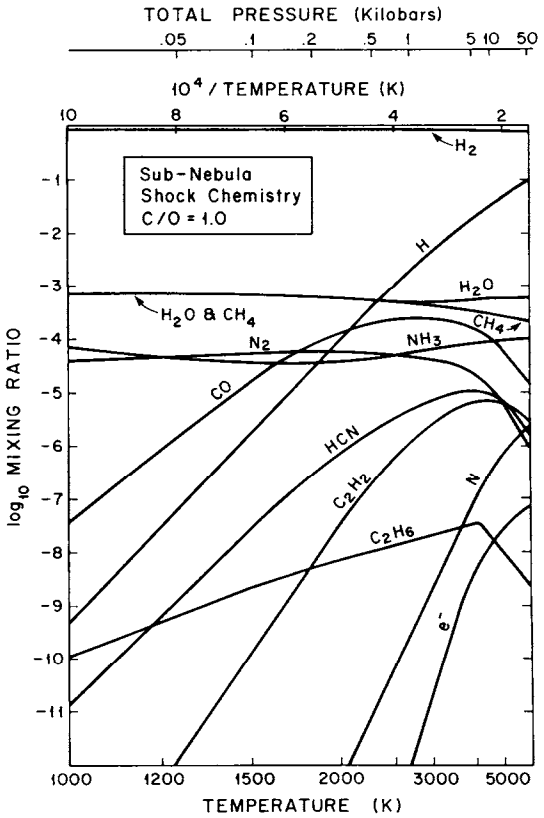

Fig. 10. As in Fig. 9 but for an initially cool, H_2O-depleted (by condensation) gas parcel which is shock heated by a lightning discharge in the outer region of the Jovian subnebula. The much higher total pressures along the assumed adiabatic P,T profile suppress molecular dissociation and ionization in comparison to the results illustrated in Fig. 9.

profile of an initially cool, H_2O-depleted (due to condensation) gas parcel in the outer regions of the hypothesized Jovian subnebula (see Fig. 10).

The maximum HCN concentrations produced by the adiabatic shock heating of nebular gases in these two different environments occur near temperatures of 3000 to 4000 K where ~ (0.2 to 6) × 10^{18} HCN molecules are formed per mole of shocked gas. These concentrations correspond to *maximum* conversions of ~ 0.3% (solar nebula) and ~ 6.5% (Jovian subnebula) of the total nitrogen abundance into HCN. In the absence of a quantitative theory for lightning discharges (and their associated shock chemistry) in the solar nebula, it is instructive to use these maximum concentrations to deduce upper limits for HCN production efficiencies by lightning discharges.

If we (initially) neglect the dissociation of H_2 to H, the energy required for the reversible adiabatic heating and compression of H_2-rich nebular gas is

given approximately by $\int C_v dT$ where C_v is the constant volume heat capacity of ideal $H_2(g)$. This energy is $\sim$ 70 to 100 kJ mole^{-1} for heating of cold ($T \sim$ 100 K) H_2-rich gas to the temperatures of 3000 to 4000 K that yield high HCN abundances (see Figs. 9 and 10). By contrast, reversible isobaric heating requires slightly more energy ($\int C_p dT \sim 90 - 120$ kJ mole^{-1}) for heating to the same temperatures. These two extremes bracket other possible (P,T) paths (e.g., isopycnic and Hugoniot) for shock heating by lightning.

Dissociation of H_2 to H requires another $\sim$ 460 kJ per mole of H_2 dissociated. As illustrated by Figs. 9 and 10, H_2 dissociation is more important at the lower pressures commonly assumed for the solar nebula than at the higher pressures assumed for the Jovian subnebula. Furthermore, ionization of $H \rightarrow H^+ + e^-$ does not appear to be significant in either environment in the 3000 to 4000 K range. Thus, energies of $\sim$ 300 kJ mole^{-1} appear to be required for heating solar nebula gas to $\sim$ 3000 K (where for this (P,T) path H_2 is $\sim$ 50% dissociated to H) and energies of $\sim$ 110 kJ mole^{-1} appear to be required for heating Jovian subnebula gas to $\sim$ 4000 K (where along this (P,T) path H_2 is only a few percent dissociated to H).

The shock heating of 1 mole of nebular gas per m^2 per year thus requires a lightning energy flux ϕ on the order of 10^{-3} J m^{-2} s^{-1}; the estimates of ϕ deduced in Sec. II.B suggest that processing of 1 mole m^{-2} yr^{-1} is probably a reasonable upper limit for outer nebular regions. The corresponding *maximum* HCN yields of $\sim (0.2 - 6) \times 10^{18}$ molecules m^{-2} yr^{-1} yield *upper limits* to the HCN production efficiencies on the order of $\sim 10^{13}$ to 10^{14} molecules J^{-1}. For comparison the NO production efficiencies in terrestrial lightning discharges are on the order of 10^{16} molecules J^{-1} (Borucki and Chameides 1984) and organic matter production efficiencies in laboratory sparking experiments on $CH_4 - NH_3 - H_2$ mixtures (see, e.g., Miller 1955) are $\sim 10^{13}$ to 10^{15} molecules J^{-1} (10^{-7} g J^{-1}) for assumed product mean molecular weights of 10^4 to 10^2. Thus, lightning discharges in the solar nebula are probably less efficient sources of disequilibrium molecules (e.g., HCN) than terrestrial lightning or laboratory discharges. However, in the cool, thermochemically inactive outer regions of the solar nebula (where their disequilibrium products may be able to accumulate without rapidly being mixed inward to high-temperature regions where reequilibration can occur), lightning discharges may be a significant source of disequilibrium material. The production of HCN with its C $\equiv$ N bond and potential for further reaction to form more complex organic molecules (Oro and Kimball 1961; Abelson 1966) is especially interesting in this regard.

(iv) Thermochemical Equilibrium/Disequilibrium for H_2O. Latimer (1950) and Urey (1952) both suggested that hydrated silicates were probable substances for retaining water in the solid planetary-forming materials that accreted to form the Earth and the other terrestrial planets. However, the lack of accurate thermodynamic data prevented them from calculating the stability

fields of hydrous silicates in the solar nebula. Despite this limitation, Urey (1952,1953) did calculate the thermodynamic conditions required for water retention as brucite $Mg(OH)_2$, water ice, and $NH_3 \cdot H_2O(s)$. This led him (Urey 1953) to conclude " that water and ammonia would have condensed in the solar nebula and the existence of the carbonaceous chondrites containing up to 10% of water confirms this conclusion . . ." However, the kinetic inhibition of the $N_2 \rightarrow NH_3$ conversion in the solar nebula, which was discussed earlier, will modify Urey's original prediction of $NH_3 \cdot H_2O(s)$ condensation.

More recent thermochemical calculations of the stabilities of H_2O-bearing phases in the solar nebula are presented in Table III and Fig. 11. These results illustrate that minor H_2O-bearing phases such as tremolite [$Ca_2Mg_5Si_8O_{22}(OH)_2$], Na-phlogopite [$NaMg_3\ AlSi_3O_{10}\ (OH)_2$], and hydroxyapatite [$Ca_5(PO_4)_3OH$] become stable in the 460 to 500 K temperature range. However, these minerals are seldom, if ever, observed in chondritic meteorites. On the other hand, major H_2O-bearing phases, which are observed in chondritic meteorites, exemplified by serpentine [$Mg_3Si_2O_5\ (OH)_4$], talc [$Mg_3Si_4O_{10}(OH)_2$], and brucite [$Mg(OH)_2$], do not become stable until temperatures of 400 K or below. However, significant formation of hydrous phases at these low temperatures in the solar nebula requires solid-solid (or gas-solid) chemical equilibrium to be approached during the lifetime of the nebula. Is this requirement satisfied or is attainment of equilibrium impossible at the (P,T) conditions where the major H_2O-bearing minerals are stable?

The formation of hydrated silicates by solid-solid reactions such as

$$\underset{\text{forsterite}}{Mg_2SiO_4} + \underset{\text{enstatite}}{MgSiO_3} + 2H_2O(g) = \underset{\text{serpentine}}{Mg_3Si_2O_5\ (OH)_4} \qquad (34)$$

requires the diffusion of Mg and Si between olivine and pyroxene at temperatures of 200 to 400 K. The characteristic diffusion time for this process can be estimated using the scaling relationship $t \sim r^2/D$ where r is the grain radius, D is the diffusion coefficient (cm^2s^{-1}), and t is the characteristic diffusion time. Freer (1981) has pointed out that under *dry* conditions, such as those expected in the solar nebula where $X_{H_2O} \leq 5 \times 10^{-4}$, divalent cations (e.g., Mg^{2+}, Fe^{2+}) in silicates generally diffuse faster than Si^{4+}. He further states that divalent cation diffusion in olivine is faster than in pyroxene.

In order to estimate the characteristic diffusion time for Mg and Si diffusion between olivine and pyroxene, which is the rate limiting step for hydrated silicate formation via reactions such as Eq. (34), we therefore make the following generous assumptions. First, we assume that both silicate reactants are in intimate contact (e.g., in the same grain) for long time periods. Second, we assume that the composite silicate grains are monodisperse, spherical grains with radii of 0.1 μm. This radius is comparable to the size of the very fine-grained matrix found in chondritic meteorites, but is significantly smaller than the size of the majority of silicate grains observed in chondrules. Third,

we assume that the diffusion of Mg and Si between olivine and pyroxene is as rapid as divalent cation diffusion in olivine. Following Cohen et al. (1983), we take the data of Misener (1974) to model Fe − Mg diffusion in olivine. This diffusion coefficient is $D \sim 6.3 \times 10^{-3} \exp(-28{,}780/T)$ $cm^2 s^{-1}$. We note that our assumptions all maximize the calculated diffusion rate and thus minimize the calculated diffusion time.

Despite these favorable assumptions, the characteristic diffusion time is estimated to be $\sim 10^{23}$s at 400 K, increasing to $\sim 10^{55}$ s at 200 K. These times are many orders of magnitude greater than the lifetime of the solar nebula ($\sim 10^{13}$ s) and the age of the solar system ($\sim 10^{17}$ s). It is easy to increase these characteristic diffusion times by making more realistic (and inherently less favorable) assumptions regarding silicate grain size and cation diffusion rates. Indeed, the assumed silicate grain radius of 0.1 μm, while comparable to the size of very fine-grained meteorite matrix and of olivines and pyroxenes found in interplanetary dust particles (e.g., see Peck 1983,1984; MacKinnon and Rietmeijer 1987), is significantly smaller than the size of the silicates commonly found in chondrules (grain size ≈ 10 to 100 μm). Furthermore, cation diffusion in pyroxene is significantly slower than cation diffusion in olivine (e.g., see Freer 1981). However, it is virtually impossible to decrease the estimated characteristic diffusion times.

Thus it is almost certain that reactions such as Eq. (34), which have been postulated for hydrated silicate formation in the solar nebula, simply do not have enough time to reach equilibrium because solid state diffusion is far too slow. As a consequence, the vapor phase hydration of monomineralic silicate grains, exemplified by the reactions

$$\underset{\text{forsterite}}{2Mg_2SiO_4} + 3H_2O(g) = \underset{\text{serpentine}}{Mg_3Si_2O_5(OH)_4} + \underset{\text{brucite}}{Mg(OH)_2} \qquad (35)$$

$$\underset{\text{enstatite}}{4MgSiO_3} + 2H_2O(g) = \underset{\text{talc}}{Mg_3Si_4O_{10}(OH)_2} + \underset{\text{brucite}}{Mg(OH)_2} \qquad (36)$$

may be the only kinetically feasible pathway for forming hydrated silicates in the solar nebula. However, as Table III and Fig. 11 show, formation of serpentine + brucite or of talc+ brucite via reaction (35) or (36) requires temperatures of ~ 200 to 300 K. The possible kinetic inhibition of gas-solid reactions at these low temperatures will now be considered.

The initial rate of reaction of water vapor with anhydrous silicate grains will depend on the collision rate of the H_2O molecules with the grain surfaces. This rate is given by

$$\sigma_w = 2.635 \times 10^{25} [P_w/(M_w T)^{1/2}] \qquad (37)$$

where σ_w has units of $cm^{-2}s^{-1}$, P_w is the water vapor partial pressure, M_w is the molecular weight of water vapor, and T is temperature. The total number

TABLE III

Predicted H_2O-Bearing Phases Stable at Thermochemical Equilibrium in Solar Nebula Gas ($T \geq$ ice condensation point)[a]

Equilibration Temperature (K)	H_2O-Bearing Phase(s)	H_2O Content (w/o)	Reference
~500	Tremolite [$Ca_2Mg_5Si_8O_{22}(OH)_2$]	2.2	Lewis 1972*a*, *b*
<470[b]	Na – Phlogopite [$NaMg_3AlSi_3O_{10}(OH)_2$]	4.5	Hashimoto and Grossman 1987
~460[c]	Hydroxyapatite [$Ca_5(PO_4)_3OH$]	1.8	Fegley and Lewis 1980
~400[d]	Serpentine [$Mg_3Si_2O_5(OH)_4$]	13.0	Lewis 1974*a*
~230[d,e]	Serpentine [$Mg_3Si_2O_5(OH)_4$]	13.0	Barshay 1981
<274[f]	Serpentine [$Mg_3Si_2O_5(OH)_4$] + Brucite [$Mg(OH)_2$]	16.1	Hashimoto and Grossman 1987
~225	Serpentine [$Mg_3Si_2O_5(OH)_4$] + Brucite [$Mg(OH)_2$]	16.1	this work
~400[d]	Talc [$Mg_3Si_4O_{10}(OH)_2$]	4.8	Lewis 1972*a*, *b*
~340[d,e]	Talc [$Mg_3Si_4O_{10}(OH)_2$]	4.8	Barshay 1981
~160 – 280[g]	Talc [$Mg_3Si_4O_{10}(OH)_2$]	4.8	Larimer and Anders 1967
~250	Talc [$Mg_3Si_4O_{10}(OH)_2$] + Brucite [$Mg(OH)_2$]	8.3	this work
~160[h]	Water Ice [H_2O]	100	Lewis 1972*a*, *b*

[a]The temperatures listed are the highest temperatures at which the H_2O-bearing phase is stable along the illustrative solar nebula (P, T) profile in Fig. 11.

[b]Na-phlogopite forms at ~470 K at 10^{-3} bar total pressure (Hashimoto and Grossman 1987). It will form at slightly lower temperatures along the (P, T) profile shown in Fig. 11.

[c]The water content is calculated on the basis of 1 H_2O molecule per 2 hydroxyapatite molecules.

[d]These calculations assume solid-solid chemical equilibrium. However, the extremely slow rate of solid state diffusion at these low temperatures probably prevents the attainment of equilibrium over the lifetime of the solar nebula. See Sec III. B(iv) of the text for a discussion.

[e]Barshay's results are reproduced in Fig. 12 of Prinn and Fegley (1987*a*). He used a feldspar-nepheline silica buffer at $T < 600$ K in these calculations.

[f]Hashimoto and Grossman (1987) calculate that serpentine + brucite form at 274 K at 10^{-3} bar total pressure. This assemblage will form at lower temperatures along the (P, T) profile shown in Fig. 11.

[g]Larimer and Anders (1967) list 2 possible talc formation reactions: $3MgSiO_3 + SiO_2 + H_2O(g) \rightarrow Mg_3Si_4O_{10}(OH)_2$ and $3Mg_2SiO_4 + 5SiO_2 + 2H_2O(g) \rightarrow 2Mg_3Si_4O_{10}(OH)_2$ with condensation temperatures in the 160 to 280 K range for total pressures of $\sim 10^{-6}$ to $\sim 10^{-3}$ bar.

[h]The shaded region for H_2O (ice, liquid) in Fig. 11 illustrates the range of condensation temperatures assuming all carbon is CH_4 or CO for total pressures of 10^{-7} to 10^2 bar.

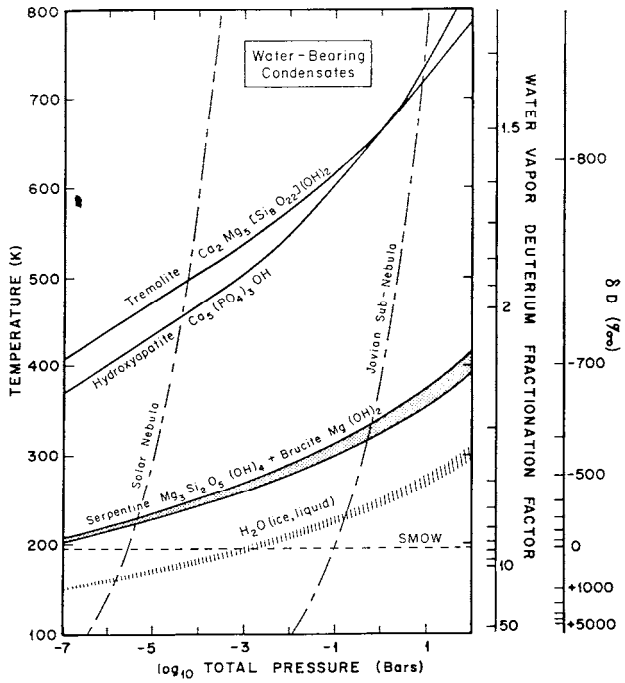

Fig. 11. The calculated stability fields for water-bearing condensates over a wide range of total pressures applicable to the solar nebula and giant planet subnebulae. The tremolite and hydroxyapatite curves are from Lewis (1974*a*) and Fegley and Lewis (1980). The serpentine + brucite curve represents hydration of forsterite by water vapor via reaction (35). The *P,T* profiles for the solar nebula and the Jovian subnebula are the same as shown in previous figures. The shaded regions for H_2O (ice, liquid) and serpentine + brucite illustrate the range of condensation temperatures if all carbon is present as CH_4 (top edge) or if all carbon is present as CO (lower edge). The amount of oxygen incorporated into *anhydrous* rock (MgO + SiO_2) is also taken into account. Equilibrium fractionation factors (Richet et al. 1977) for temperature-dependent deuterium partitioning between HD(*g*) and $H_2O(g)$ are also shown. These are independent of the absolute D/H ratio in either phase. Deuterium is enriched in H_2O (relative to HD) with decreasing temperature. However, δD = [(D/H)water - (D/H)SMOW]/[(D/H)SMOW] x 1000 where SMOW = standard mean ocean water with D/H = 1.557×10^{-4} (Pillinger 1984) depends on the absolute D/H value chosen for H_2 in the solar nebula. Following Cameron (1982), this is taken as 2.0×10^{-5}. Both the heterogeneous gas-solid equilibration of $H_2O(g)$ with anhydrous minerals (to form hydrous phases) and the homogeneous gas phase isotopic equilibration of $H_2O(g)$ and HD(*g*) are problematic at low temperatures and rapid mixing rates (i.e., short mixing times) in the solar nebula.

of collisions with all forsterite (or enstatite) grains in each cm^3 of the nebula is given by

$$\nu_w = \sigma_w A \tag{38}$$

where ν_w has units of $cm^{-3}s^{-1}$ and A is the total surface area of all forsterite (or enstatite) grains in each cm^3 of the nebula. The grains are assumed to be

monodisperse, spherical grains which are uniformly distributed at solar abundance in the gas. The present calculations also assume a grain radius of 0.1 μm consistent with the earlier diffusion calculations.

The collision time constant t_{coll} for water molecules to collide with forsterite (or enstatite) grains in each cm^3 of the nebula is then

$$t_{coll} \sim [H_2O]/\nu_w \tag{39}$$

where $[H_2O]$ is the molecular number density of water vapor. This abundance is taken as the stoichiometric amount of water vapor required for hydrated silicate formation ($\sim$ 20% of the total H_2O molecular number density). If every collision led to silicate hydration, Eq. (39) would also be the expression for the chemical time constant t_{chem}. However, only a small fraction of collisions which possess the necessary activation energy lead to hydration. This fraction is given by

$$f_w \sim \nu_w \exp(-E_a/RT) \tag{40}$$

where E_a is the activation energy and R is the ideal gas constant. The chemical time constant t_{chem} for silicate hydration is thus given by

$$t_{chem} \sim [H_2O]/f_w \sim t_{coll}/\exp(-E_a/RT). \tag{41}$$

Figure 12 illustrates the collision time constant t_{coll} for reaction (35), which exemplifies the vapor phase hydration of anhydrous silicates. The amount of H_2O that can be incorporated into serpentine + brucite ($\sim$ 20% of available water vapor in the CO-rich solar nebula) collides with 0.1 μm radius forsterite grains in less than an hour; this time increases linearly with the assumed grain radius. However, because only a small fraction of the collisions actually leads to chemical reaction, the chemical time constant t_{chem} is significantly longer than the collision time constant. In the absence of experimental data on the low pressure vapor phase hydration of forsterite, we utilize the results of Layden and Brindley (1963) and Bratton and Brindley (1965) on the vapor phase hydration of MgO to $Mg(OH)_2$ (which has an activation energy $\sim$ 70 kJ $mole^{-1}$) in order to estimate t_{chem} for the vapor phase hydration of forsterite.

The estimated t_{chem} for forsterite hydration, which is displayed in Fig. 12, is $>10^4$ times longer than the solar nebula lifetime (i.e., $t_{chem} > 10^{17}$s) at the temperature ($\sim$ 225 K) where forsterite hydration to serpentine + brucite becomes thermodynamically favorable. Furthermore, this t_{chem} value should be regarded as a lower limit to the lifetimes (and thus an upper limit to the rates) for silicate hydration reactions in the solar nebula because reactions requiring the migration and diffusion of more than one metal cation will probably proceed slower than MgO hydration which involves only one metal cation. Thus, formation of serpentine, talc, brucite and of other related hydrous

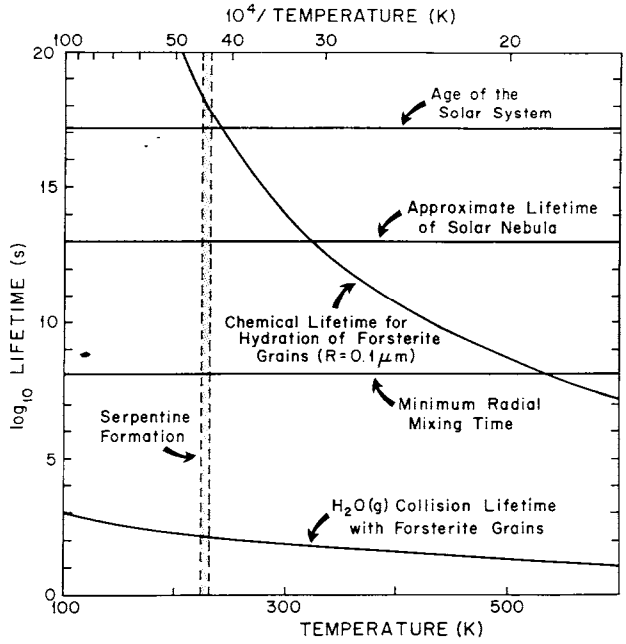

Fig. 12. Chemical and physical lifetimes associated with the hydration of forsterite Mg_2SiO_4 grains by $H_2O(g)$ to form serpentine $Mg_3Si_2O_5(OH)_4$ in the solar nebula. All Mg is assumed to be present in forsterite, which is a proxy for the more diverse suite of Mg- bearing minerals present in the solar nebula at low temperatures (e.g., see Barshay 1981). The assumed (spherical, monodisperse) forsterite grain diameter of 0.2 μm is consistent with the observations of 30 μm x 5 μm olivine plates and micron-sized olivine grains in C3V meteorite matrix (Peck 1983, 1984), which is believed to be a mixture of (relatively) unaltered nebular materials (McSween 1979*a*). The assumed grain size is also consistent with observed grain sizes for olivine and pyroxene in interplanetary dust particles (MacKinnon and Rietmeijer 1987). However most silicate grains found in chondrules in meteorites are significantly larger than 0.2 μm and thus will react significantly slower than the smaller assumed 0.2 μm grains. The shaded region for serpentine illustrates the range of condensation temperatures if all carbon is present as CH_4 (slightly higher T) or if all carbon is present as CO (slightly lower T). Note that the chemical lifetime for forsterite hydration (assuming it is as energetically favorable as MgO hydration) is longer than the lifetime of the solar nebula. Consequently, formation of serpentine (as well as talc and brucite which form at a similar temperature) is very probably kinetically inhibited.

minerals forming at these low temperatures $\leq$ 300 K is probably kinetically inhibited. The implications of this kinetic inhibition for water retention by the terrestrial planets, chondritic meteorites and asteroids will be examined in Sec. IV.

(v) Low temperature condensation. The nature of low temperature condensates (e.g., ice, hydrates, clathrates, etc.) in the nebula and subnebulae

depends sensitively on the degree of disequilibration for carbon, nitrogen and oxygen compounds. In particular, depending on the quench temperature T_Q for the $CO \rightarrow CH_4$ and $N_2 \rightarrow NH_3$ conversions (see Sec. III.B (i) above) we can proceed from the (low T_Q) *equilibrium* sequence (H_2O, $NH_3 \cdot H_2O$, $CH_4 \cdot 6H_2O$, etc.) to the (high T_Q) *disequilibrium* sequence (NH_4HCO_3, H_2O, NH_4COONH_2, CO_2, $CO \cdot 6H_2O$, $N_2 \cdot 6H_2O$, etc.). As already noted we expect the *disequilibrium* sequence in the solar nebula and the equilibrium sequence in protoplanetary subnebulae.

These two general sequences are further complicated in the solar nebula (but not in subnebulae) by probable catalytic conversion of CO to light and heavy hydrocarbons (Sec. III.B (ii)) and by probable kinetic inhibition of hydrated silicate formation (Sec. III.B (iv)). Catalytically formed hydrocarbons provide a mechanism for retention of cosmically important amounts of carbon at temperatures well above the $CO \cdot 6H_2O$ condensation point, while catalytically formed hydrocarbons and kinetic inhibition of silicate hydration lead to an increase in the H_2O/silicate (ice/rock) ratio (through conversion of $CO \rightarrow H_2O$ or prevention of $H_2O \rightarrow$ silicate OH).

A summary of the major low-temperature condensation sequences is provided in Table IV. The dramatic differences in the predicted condensation sequences in the solar nebula and the planetary subnebulae mean that certain volatile compound ratios (e.g., N_2/NH_3, CO/CH_4, H_2O ice/rock) may be diagnostic of origin for ice-rich bodies. We will address this point specifically in our discussion of ice-rich satellites and comets in the next section.

IV. IMPLICATIONS FOR SPECIFIC OBJECTS

A. Terrestrial Planets

The large depletions of the nonradiogenic rare gases relative to other, chemically reactive volatiles on the surface of the Earth (e.g., see Brown 1949) has led to the generally accepted hypothesis that the volatiles on Venus, Earth and Mars are almost entirely secondary and did *not* originate principally by gas capture from the solar nebula. Instead, the volatile endowments on the terrestrial planets are the result of chemical processes (e.g., for C, N and H_2O) and physical processes (e.g., for the rare gases) for retaining volatiles in solid grains. These volatile-bearing grains were either accreted in an essentially homogeneous fashion along with the bulk of planetary-forming materials or were delivered in an essentially inhomogeneous fashion to the terrestrial planets after they had finished (or were near the end of) their accretion. Some of the consequences of a simple two component inhomogeneous accretion model for planetary volatiles are discussed by Wänke (1981) and the chapter by Dreibus and Wänke.

The radial temperature gradient in the solar nebula was a major influence on the nature and abundance of the volatile-bearing grains. For the unlikely

TABLE IV
Low Temperature Condensation Sequences Predicted in the Protosolar Nebula and Protoplanetary Subnebulae*

Protosolar Nebula		Protoplanetary Subnebula
CO-rich	**CO plus Hydrocarbons**	
Largely anhydrous rock	Largely anhydrous rock Involatile carbonaceous compounds[a,b]	Largely hydrated rock
H_2O (150 K)	H_2O	H_2O (235 K)
NH_4HCO_3/NH_4COONH_2 (150, 130 K)[a]	NH_4HCO_3/NH_4COONH_2[a] Light hydrocarbons and hydrocarbon clathrates[c]	$NH_3 \cdot H_2O$ (160 K) $CH_4 \cdot 6H_2O$ (94 K)
CO_2 (70 K)[a]	CO_2[a]	CO (20 K)[a]
$CO \cdot 6H_2O$ (60 K)[d]	$CO \cdot 6H_2O$[d]	N_2 (20 K)[a]
$N_2 \cdot 6H_2O$ (55 K)[d]	$N_2 \cdot 6H_2O$[d]	
CO (20 K)	CO (20 K)	
N_2 (20 K)	N_2 (20 K)	

[a]These compounds contain $\leq 10^{-2}$ of the total C or N.
[b]Exemplified by organic material in chondrites, and formed by nebular Fischer-Tropsch-type reactions and/or of interstellar origin.
[c]Exemplified by the light ($C_1 - C_5$) hydrobarbons formed as initial products in high H_2 : CO environments (see Fig. 8). Precise condensation or enclathration temperature depends on the chain length and hydrocarbon abundance.
[d]There is insufficient H_2O to allow condensation of all C and N as CO and N_2 clathrates.
*Condensation temperatures in illustrative models (Lewis and Prinn 1980; Prinn and Fegley 1981*a*) are given for each condensate where available. For the nebula the "CO plus hydrocarbons" sequence is preferred with the condensation temperatures being slightly below those in the CO-rich case (the precise temperatures will depend on the degree of CO to hydrocarbon conversion).

case in which chemical equilibrium was completely maintained with decreasing temperature, the solid grains equilibrated at lower temperatures (i.e., farther from the proto-Sun) would be more volatile rich than the solid grains equilibrated at higher temperatures (i.e., closer to the proto-Sun). However, more plausibly, if chemical disequilibrium prevailed with decreasing temperature, processes such as Fischer-Tropsch-type reactions and lightning-induced shock heating would become more important and build up reservoirs of volatile-rich disequilibrium material. In turn, transport of such volatile-rich disequilibrium material inward to higher temperature regions would lead to its pyrolysis and to the eventual production of volatile-poor grains.

We also note that for both equilibrium and disequilibrium scenarios, decreasing temperatures may have allowed important exceptions to this general behavior. For example, if chemical equilibrium prevailed, the amounts of elemental carbon and nitrogen dissolved in Fe – Ni alloy would have gone through maxima in the inner regions of the solar nebula (see Figs. 13 and 14). On the other hand, if disequilibrium prevailed, decreasing temperatures would have kinetically inhibited water retention by solid grains (Fig. 12) or may

have halted production of organic matter by deactivation of an essential catalyst (e.g., formation of FeS coatings on Fe particles at ~ 680 K).

A comparison of the observed C, N and H_2O inventories on Venus, Earth and Mars with the predicted inventories deduced using the idealized assumptions of complete chemical equilibrium and complete degassing of volatiles provide insight into the maximum contributions of equilibrium processes to the volatile inventories of these planets. This comparison is presented in Table

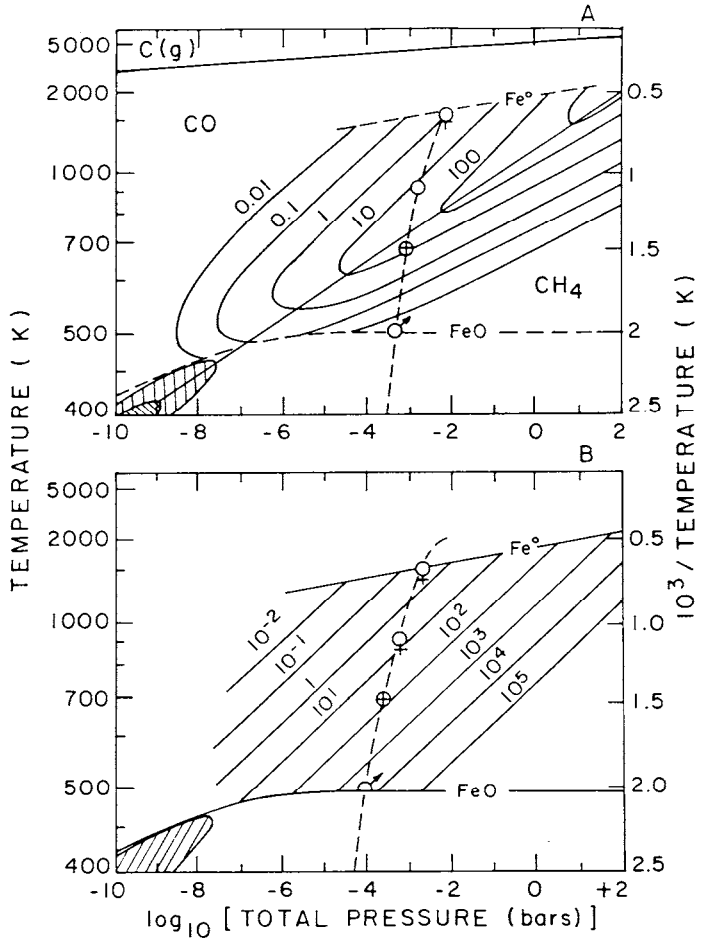

Fig. 13. Predicted concentrations (parts per million by mass) of elemental carbon dissolved in Fe - Ni alloy equilibrated with solar nebula gas. The assumed solar nebula *P,T* profile is also shown as a dashed line with the astrological symbols for Mercury, Venus, Earth and Mars from top to bottom. The predicted bulk carbon contents for Venus, Earth and Mars are calculated using metal contents from models *V2*, *E5*, and *Ma2* from the *Basaltic Volcanism Study Project* (1981*b*, p. 641). (A) Complete thermochemical equilibrium between CO and CH_4 and all other species is maintained. (B) Kinetic inhibition of the CO → CH_4 conversion (figure after Lewis et al. 1979 and Lewis and Prinn 1980).

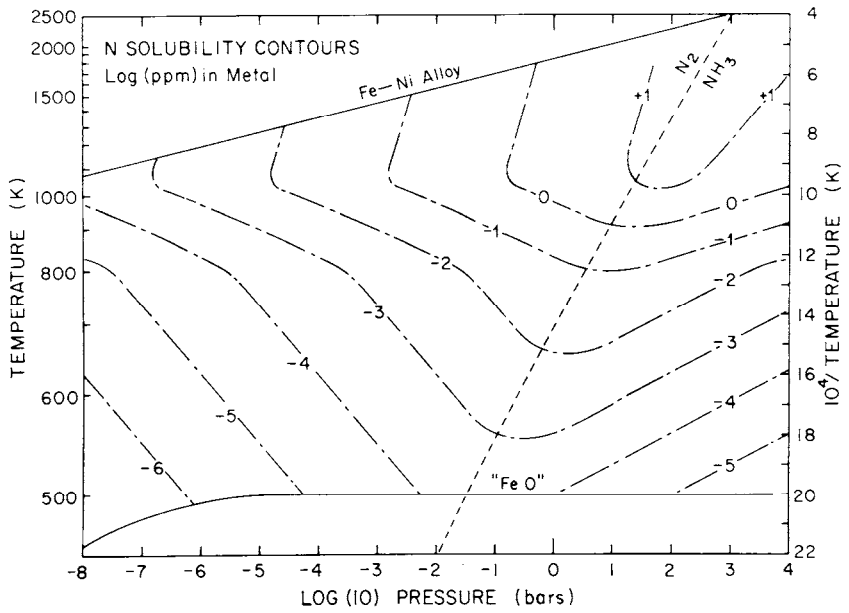

Fig. 14. Predicted amounts (parts per million by mass) of N dissolved in Fe - Ni alloy equilibrated with solar nebula gas (figure from Fegley 1983). Bulk nitrogen contents are calculated using the planetary composition models (for wt. % metal) given in the caption to Fig. 13.

V, where volatile inventories are tabulated on an absolute basis (g/g). Several trends are immediately apparent.

First, addressing carbon, we see that although the observed carbon inventories are approximately similar for Venus and the Earth, the bulk inventories predicted for maintenance of chemical equilibrium (between CO, CH_4, and Fe − Ni grains) decrease from Venus to Earth. The predicted inventories are also lower than the observed inventories for both Venus and the Earth. The observed carbon inventory on Mars (atmospheric CO_2), which is certainly a lower limit to the bulk inventory, is also larger than the predicted equilibrium value. Furthermore, since the degassing efficiency for carbon which is dissolved in Fe − Ni alloy is probably much less than 100%, the already significant discrepancies between the observed inventories and the (lower) predicted values will be increased.

However, as discussed previously in Sec. III.B, the $CO \rightarrow CH_4$ conversion was kinetically inhibited in the solar nebula (Fig. 2). As shown in Fig. 13, this leads to much larger amounts of elemental carbon dissolved in Fe − Ni alloy in the (P,T) region where CH_4(g) is thermodynamically stable (but kinetically inhibited from forming). In this case, the predicted carbon inventory for Venus remains the same while those for Earth and Mars are increased

TABLE V

Comparison (g/g) of Observed H_2O, C and N Volatile Inventories of Venus, Earth and Mars with Predictions of the Complete Equilibrium and Kinetic Inhibition Models[a]

Volatile	Venus		Earth		Mars	
	atmo.	bulk	atmo.	bulk	atmo.	bulk
CO_2 (obs.)	10^{-4}		4×10^{-10}	8×10^{-5}	4×10^{-8}	
(pred.)[b]		2×10^{-5}		$(0.07 - 3) \times 10^{-4}$		$(0.0001 - 8) \times 10^{-5}$
N_2 (obs.)	2×10^{-6}		6×10^{-7}	3×10^{-6}	7×10^{-10}	
(pred.)		4×10^{-9}		3×10^{-11}		10^{-13}
H_2O (obs.)	4×10^{-9}		5×10^{-9}	3×10^{-4}	5×10^{-12}	
(pred.)		0		10^{-5}		8×10^{-3}

[a]Atmospheric inventories based on Tables 2-4 of Prinn and Fegley (1987*a*). Terrestrial bulk inventory based on Table I. Note that this table is not normalized to Si and is simply on a (g/g) basis.

[b]Predictions based on Barshay (1981), and Figs. 13 and 14. The range of CO_2 values for Earth and Mars results from including (highest values) or excluding (lowest values) the effects of kinetic inhibition on dissolved carbon in grains.

over the equilibrium values. Indeed, depending on the extent to which CO(g) − Fe,Ni grain equilibrium is maintained with decreasing temperature and on the maintenance of the Fe − FeO equilibrium, Mars may have been endowed with as much (or more) carbon than the Earth.

Chemical analyses of the SNC (Shergottite-Nakhlite-Chassigny) meteorites, which are widely believed to come from Mars (reviewed by Laul 1986), may be instructive in constraining the bulk Martian carbon inventory. Although the carbon contents of the shergottite meteorites studied by Wright et al. (1986) were variable, the values found of $\sim 2 \times 10^{-5}$ to $\sim 6 \times 10^{-4}$g/g are much greater than the predicted equilibrium value for Mars but are compatible with those predicted from this CO/CH_4 disequilibrium scenario. The problem of degassing the carbon from the Fe − Ni alloy remains, however. Thus, while carbon dissolved in Fe − Ni alloy may have played some role in delivering carbon to the terrestrial planets, the probability of the Fischer-Tropsch-type reactions discussed in the previous section and the considerable evidence for ubiquitous organic material in the solar nebula discussed later in this section make organic material an equally probable source of carbon for Venus, Earth and Mars.

Second, addressing nitrogen, we see from Table V that the observed N_2 inventories for Venus, Earth and Mars are all significantly greater than the N_2 inventories predicted for $N_2(g)$ − Fe,Ni grain equilibrium in the solar nebula (Fig. 14). Again, degassing efficiencies $< 100\%$ will increase the large discrepancies between the observed inventories and the predicted values. Kinetic inhibition of the $N_2 \rightarrow NH_3$ conversion in the solar nebula does not alter this situation because the N_2/NH_3 ratios are much greater than unity for typical nebular pressures down to $\sim$ 400 K where Fe_3O_4 coatings will stop further nitrogen solution in the metal.

However, the nitrogen inventories of the terrestrial planets could have been supplied by other equilibrium sources. The highly reduced enstatite chondrites contain metal nitrides such as TiN (osbornite) and Si_2N_2O (sinoite); these minerals and other nitrides are also predicted to form in a solar gas having C/O ratios greater than the solar value of $\sim$ 0.6 (Larimer and Bartholomay 1979). Accretion and degassing of only a trace amount of these materials (e.g., of all Zr as ZrN giving N $\sim 9 \times 10^{-7}$ g/g or of $\sim$ 1% of all Ti as TiN giving N $\sim 2 \times 10^{-6}$ g/g in chondritic material) is sufficient to supply the observed nitrogen inventories on Venus and the Earth.

Alternatively, just as for carbon, accretion and degassing of a small amount of N-bearing disequilibrium organic material similar to that found in carbonaceous chondrites (e.g., see Hayatsu and Anders 1981) can also supply the nitrogen inventories on these planets. In this regard, we note that even the small amount of NH_3 predicted to be present in the solar nebula is more than sufficient to provide the amounts of nitrogen on the Earth and Venus. In fact, for $NH_3/N_2 \sim 2 \times 10^{-3}$ (which assumes Fe catalysis of the $N_2 \rightarrow NH_3$

conversion down to 480 K), accretion of only ~ 1% of this NH_3 as N-bearing organics will provide the required amounts of nitrogen in chondritic material. Hayatsu and Anders (1981) describe experiments showing NH_3 incorporation into organic material via Fischer-Tropsch-type reactions.

Third, examining H_2O in Table V, we see that increasing amounts of water are predicted to be retained in solid grains in the unlikely event that $H_2O(g)$-silicate grain equilibrium is maintained with decreasing temperature. Furthermore, the well known equilibrium fractionation of deuterium from HD to HDO (via the net reaction $HD + H_2O = H_2 + HDO$) with decreasing temperature (e.g., see Urey 1947) means that the D/H ratio of this bound water is also predicted to increase with decreasing temperature. This is illustrated in Fig. 11. The equilibrium model thus predicts that the Earth accreted significantly more hydrated phases (e.g., tremolite, hydroxyapatite, phlogopite, talc, serpentine) than did Venus because these phases only became thermodynamically stable in the cooler nebular region outside of 1 AU. Furthermore, Mars is predicted to have accreted even more of the hydrated minerals than the Earth did and is predicted to be even more water rich and more D rich. The (inferred) presence (by infrared reflection spectroscopy) of hydrated phases on the surface of the asteroid 1 Ceres (Lebofsky 1978), the (inferred) presence of abundant water on Mars (Carr 1987), and the larger than terrestrial D/H ratio on Mars (Owen et al. 1987), are in qualitative agreement with this trend but certainly are not unambiguous evidence in support of the equilibrium model. In particular, the higher than terrestrial D/H ratio on Mars may be due to D/H fractionation during hydrogen escape from Mars (Yung et al. 1987*b*).

The observation of D/H ~ 1.6×10^{-2} on Venus, measured by the Pioneer Venus mass spectrometer (Donahue et al. 1982), poses a potential problem for this equilibrium model of water retention. The observed D/H value, which is ~ 100 times higher than the terrestrial value of 1.557×10^{-4} SMOW (standard mean ocean water), is consistent with the depletion of an amount of water equivalent to ~ 0.3% of the terrestrial water inventory from Venus over geologic time (McElroy et al. 1982*a*; Donahue et al. 1982), with the water being primordial or added by ancient cometary impacts (Grinspoon 1987). This is a small amount of water which could have been supplied to Venus by the accretion of only trace amounts of hydrated phases (e.g., accretion of only 0.04% of all Ca if present as tremolite or accretion of only 0.002% of all Mg if present as serpentine). However, more water may have initially been present since Donahue et al. (1982) note that enhancement of the D/H ratio by hydrodynamic escape will only begin once the H_2O mixing ratio drops below ~ 2×10^{-2}; this is equivalent to the 0.3% of the terrestrial inventory mentioned above.

Supplying the very large water inventories on the Earth and Mars by equilibrium material is very problematical. As illustrated in Table III and Fig.

12, formation of the major water-bearing minerals serpentine, talc and brucite in the solar nebula was apparently kinetically inhibited inside the thermodynamic stability fields of these phases. Thus, unless hydration of Ca-bearing minerals to tremolite and subsequent accretion of the tremolite occurred with combined efficiencies $\sim$ 10%, the Earth for example must have received its water from some other source. This may have been in the fashion of an inhomogeneously accreted volatile-rich veneer (Anders 1968) or from ice-rich bodies gravitationally scattered into the inner solar system.

B. Chondritic Meteorites and Asteroids

The importance of disequilibrium processes for the production and preservation of organic matter in chondritic meteorites has recently been the focus of several studies. Hayatsu and Anders (1981) have summarized the evidence for and against the synthesis of different classes of organic compounds by Fischer-Tropsch-type reactions in the solar nebula. As discussed previously, the kinetic inhibition of the $CO \rightarrow CH_4$ conversion in the solar nebula, resulting in a supersaturated carbon-bearing gas, favors organic matter production by these reactions. Some investigators have even proposed that Fischer-Tropsch-type reactions may have synthesized organic compounds in the meteorite parent bodies. Although these latter proposals remain to be studied seriously, they are not inconsistent with our earlier observation that high total conversions of CO to organics and low H_2/CO ratios are more favorable for production of large molecules than are low total conversions of CO to organics and high H_2/CO ratios (see Sec. B (ii) and Fig. 8).

Isotopic studies of organic matter and coexisting phases (e.g., carbonates and hydrated silicates) in chondrites provide additional evidence for disequilibrium processing of the major volatiles C, N and H. The pattern of ^{13}C-light organic matter and ^{13}C-heavy carbonates, which is observed in the CI1 and CM2 chondrites (e.g., see Mason 1971), was reproduced in CO_2 and hydrocarbons generated from Fischer-Tropsch reactions of $CO + H_2$ done at 400 K (Lancet and Anders 1970). Unfortunately, this promising study has not been followed up in sufficient detail to determine the effects of processing variables (e.g., temperature, total pressure, H_2/CO ratio, type of catalyst, etc.) on the resultant $^{13}C/^{12}C$ ratios in the CO_2 and organic products.

On the other hand, the ^{15}N-rich soluble organic matter found by Becker and Epstein in CI1 and CM2 chondrites is much more fractionated than N-bearing organics produced via either Fischer-Tropsch-type or Miller-Urey reactions (summarized by Pillinger 1984). However, given the extensive evidence for $^{15}N/^{14}N$ heterogeneity between (and within) meteorites (Pillinger 1984), thus suggesting nebular heterogeneity, formation of the ^{15}N-rich soluble organics from a ^{15}N-rich reservoir with little (or no) fractionation during the synthesis cannot be ruled out.

However, the most dramatic isotopic variations in meteorites are dis-

played by hydrogen and deuterium. Figure 11 illustrates the well-known point that deuterium exchange between the major deuterium-bearing reservoir in the solar nebula (HD) and gaseous hydrides (e.g., H_2O in this case but the same is true for CH_4, NH_3, etc.) does not lead to large deuterium enrichments in the hydride until sufficiently low temperatures where the gas-phase exchange reaction will be kinetically inhibited. If we take CH_4 as a proxy for organic matter, we would not expect large D/H ratios in organics unless they had equilibrated with HD at similarly low temperatures (with larger D/H ratios requiring lower temperature equilibration).

Thus, the observation of D-rich organic matter having D/H ratios up to $\sim 1.05 \times 10^{-3}$ (as compared to $\sim 2 \times 10^{-5}$ for cosmic hydrogen and $\sim 16 \times 10^{-5}$ for terrestrial hydrogen) is very significant. As discussed at length by Pillinger (1984) and Yang and Epstein (1983), matter with such large D/H ratios is almost certainly of interstellar origin. This is a plausible conclusion because apparently only ion-molecule reactions, which occur in interstellar clouds, proceed with non-negligible rates at the low temperatures ($\leq$ 100 K) required to achieve such large D/H fractionations.

The survival of this D-rich material in meteorites poses important constraints on the severity and duration of thermal processing experienced by this material after its formation. The rate of isotopic re-equilibration back to lower D/H ratios (see Fig. 11) is clearly a temperature dependent process which is coupled in important ways to the rates of nebular transport and thermal evolution. Although no models of the survivability of D-rich material are currently available, the presence of high D phases in both ordinary and carbonaceous chondrites implies the kinetic inhibition of gas-solid reactions involved in the isotopic re-equilibration over a range of (P,T) conditions in the inner nebula. Indeed, such kinetic inhibition would not be surprising given the refractory nature of these D-rich phases (which are residues left after dissolution of the bulk of the meteorite in HCl-HF solutions) and the high C-H bond strength ($\sim$ 370 – 460 kJ mole^{-1} for a variety of organic compounds).

Our earlier discussion of the kinetic inhibition of H_2O (g)-silicate hydration reactions in the solar nebula implies that the hydrated silicates observed in CI1 and CM2 chondrites are not nebular products but are instead products of hydration reactions on the chondrite parent bodies. This interpretation is in accord with the extensive petrographic evidence summarized by Barber (1985) that implies an origin for the hydrated silicates by aqueous alteration on the chondrite parent bodies. More recent work by Tomeoka and Buseck (1985) also supports this model. Furthermore, aqueous activity on the CI1 and CM2 chondrite parent bodies is also required to explain the production of sulfate- and carbonate-bearing veins (see Barber 1985). In fact, as reviewed by Pillinger (1984), unidirectional oxidation in an aqueous environment of FeS (troilite) provides a plausible explanation for the observed sulfur isotopic compositions of FeS, elemental S, and the sulfate veins. Finally, Clayton and

Mayeda (1984) have shown that the oxygen isotopic compositions of CI1 and CM2 chondrites require $T < 293$ K and H_2O (liquid) volume fractions $> 44\%$ to produce the hydrated silicates in CM2 chondrites and aqueous alteration in a warmer, wetter environment to produce the hydrated silicates in CI1 chondrites.

Thus, a large number of chemical, isotopic and petrographic observations support the theoretical interpretation that the hydrated silicates in CI1 and CM2 chondrites are parent body and *not* nebular products. The kinetic inhibition of silicate hydration reactions in the solar nebula also implies that the hydrated silicates inferred to be present on the asteroid 1 Ceres are also aqueous alteration products. This interpretation is supported by the similarities in the infrared reflection spectra of the putative hydrated silicates on 1 Ceres and the hydrated phases in carbonaceous chondrites (Feierberg et al. 1981) and the inferences that asteroids are the source of the chondritic meteorites.

However, the interesting question of how water was originally retained on the asteroids and chondrite parent bodies must then be addressed. The simplest way to do this is by condensation of water ice. Figure 11 illustrates that water ice condenses at $\sim$ 160 K along the solar nebula (P,T) profile used. This corresponds to $R \sim 3.4$ AU (near the outer edge of the present-day asteroid main belt) for the same model (Barshay 1981), which assumes $T \propto R^{-1}$ and takes $T \sim 550$ K at 1 AU. Higher nebular pressures lead to higher water ice condensation temperatures with $T \sim 200$ K at a total pressure of $\sim 10^{-3}$ bar (see Fig. 11). Assuming that HD and H_2O continued to equilibrate down to these temperatures, the implied δD (defined in the caption to Fig. 11) for the water ice (neglecting the smaller fractionation between water vapor and ice) is ~ -70 per mil for condensation at ~ 200 K up to $\sim +630$ per mil for condensation at ~ 160 K. The D/H ratio in this water ice should be reflected in the hydrated silicates in the CI1 and CM2 chondrites.

The inferred δD values for hydrated silicates in carbonaceous chondrites are ~ -100 per mil (Kolodny et al. 1980; Yang and Epstein 1983). This suggests that the precursor water ice either condensed at ~ 200 K or alternatively that HD $-$ H_2O equilibration was quenched at ~ 200 K. Thus, the available isotopic data are consistent with derivation of the hydrated silicates from water originally retained as water ice but do not rule out another (more complex) origin. We note that models of this type were first proposed by Dufresne and Anders (1962).

C. Giant Planets

Hypotheses for the origin of the giant planets generally involve either direct *collapse* of nebula gas and grains (e.g., see Cameron 1978) or *capture* of nebula gas and grains by a preformed solid core (see, e.g., Mizuno 1980). Because the directly collapsed planet can subsequently capture solid material,

both scenarios predict planets which potentially are enriched by various amounts in those elements accreted in the solid material (ices, rock). The two models are therefore often considered equivalent for explaining bulk planetary composition but *not* for explaining the distribution of elements within a planet (clearly the capture model can potentially sequester more of the heavy elements in the core if interior mixing is weak).

Jupiter and Saturn were most likely formed where nebular temperatures exceeded 60 K but were less than the water ice condensation temperature. Thus examining the "CO plus hydrocarbons" case in Table IV, the *solid* material which comprised their precursor cores and/or accreted onto the gaseous planets (via an accretion disk or otherwise) contained the full solar complement of rock-forming elements except oxygen. Oxygen would be present as silicates, hydrated silicates and water ice but depleted relative to solar abundance by the factor d_O = [total O]/([total O] − [CO]) in the surrounding solar nebula (because CO remains in the gas phase). Clearly $d_O \simeq 1$ (i.e., no significant depletion) if catalytic conversion of CO to hydrocarbons plus H_2O was facile in the nebula while $d_O \simeq$ [total O]/([total O] − [total C]) = 2.5 if catalytic conversion was inhibited. Carbon would be depleted by the factor d_C = [total C]/([total C] − [CO]) which varies from $d_C \simeq 1$ for facile CO → hydrocarbon conversion up to $d_C \simeq$ [total C]/([NH_4HCO_3] + [NH_4COONH_2]) ≈ 100 for inhibited conversion. The observations force us to reject d_C values >> 1. In particular the Jovian and Saturnian ice-plus-rock mass fractions (Sec. I.C) combined with their 2 to 5 times enhancements in CH_4/H_2 lead us to conclude that C must have comprised 9 to 39% (Jupiter) and 3 to 12% (Saturn) of the mass of the ice-plus-rock fraction. Such high C contents require that at least partial CO → condensed hydrocarbon conversion occurred. Finally nitrogen in the solids would be depleted relative to solar abundance by the factor $d_N \simeq$ [total N]/([total N] − 2[N_2]) ≃ [total N]/([NH_4HCO_3] + 2[NH_4COONH_2]) ≈ 100 (note that facile N_2 → involatile organic conversion is unlikely).

Uranus and Neptune most likely formed at temperatures below 60 K. In contrast to Jupiter and Saturn, the bulk of the mass of these planets was accreted as solid material rather than (solar-composition) gas. Fegley and Prinn (1986) have discussed a wide variety of generic models for these planets. We will focus again on the more plausible CO-plus-hydrocarbons case (see Table IV). The gas/solid ratio in material which formed Uranus as deduced from its bulk density and interior models varies from 11/89 to 25/75 by mass (Hubbard 1984*a*; Stevenson 1982*b*). To attain such ratios, enrichment factors *e* (relative to solar composition) for the ice- and rock-forming elements of 100 to 1000 are demanded. If the nebula temperature is below 20 K, then pure CO and N_2 solids will be present in the accreted condensed material and the ice/rock ratio in this material will be 2.3 (where "ice" here refers to all solids other than anhydrous rock; see Table IV). If the nebula temperature is instead

about 50 K, then only a part of the nebular CO and N_2 is condensed (as clathrates) and the ice/rock ratio in accreted condensed material will be 0.6 to 2.3 with the precise value depending on the degree of CO → hydrocarbon conversion.

An important implication of the kinetic inhibition nebular models is that if Uranus and Neptune accreted large amounts of disequilibrium C and N (e.g., carbonaceous chondrite-like organic matter or CO, CO_2, N_2 in solids and clathrates), then planetary H_2 would be depleted by reactions such as

$$C_xH_yN_z + \frac{1}{2}(3z + 4x - y)H_2 \rightarrow xCH_4 + zNH_3 \quad (42)$$

$$CO + 3H_2 \rightarrow CH_4 + H_2O \quad (43)$$

$$CO_2 + 4H_2 \rightarrow CH_4 + 2H_2O \quad (44)$$

$$N_2 + 3H_2 \rightarrow 2NH_3 \quad (45)$$

and thus the H_2/He ratio would be decreased relative to its solar value of 7.4. The maximum H_2/He ratio decrease is by a factor $\approx 1 - 0.0028(e + 1) \geq 0.7$ which applies when nebular C and N are largely in CO and N_2 and nebular temperatures are ≤ 20 K. In contrast if a significant fraction of nebular C and N is in saturated organics and/or the nebular temperature ≈ 50 K then the H_2/He ratio is much less affected.

The Uranian J_2 and ϵ values favor ice/rock ratios > 1 (Hubbard 1984*a*, and references therein) and the Uranian H_2/He ratio is not different from the solar value within the measurement uncertainties (Conrath et al. 1987; Hanel et al. 1986). This argues again that conversion of some of the CO to hydrocarbons must have proceeded in the solar nebula as suggested (but not quantified) by Lewis and Prinn (1980); more specifically, the organic carbon was at least comparable to CO in abundance. It will be interesting to see if the Neptunian H_2/He ratio leads to a similar conclusion.

D. Satellites of Giant Planets and Pluto

The condensation sequence appropriate to satellite condensation in an equilibrium solar nebula was first elucidated by Lewis (1972*a*) who demonstrated the expected ubiquity of pure water ice (H_2O) as the major condensate in the outer solar system. In agreement with the suggestions by Urey (1952) and Miller (1961), he also pointed out the potential importance of retention of nitrogen and carbon in the form of *methane clathrate* ($CH_4 \cdot 6H_2O$) and *ammonia hydrate* ($NH_3 \cdot H_2O$). The later work of Lewis and Prinn (1980) showed, however, that the equilibrium assumption in the solar nebula was incorrect and that N_2 (*not* NH_3) and CO (*not* CH_4) were the dominant gaseous nitrogen and carbon compounds. This meant that the ice/silicate ratio was

decreased from that in the equilibrium model (because CO not H_2O was the major oxygen reservoir) and also that $CH_4 \cdot 6H_2O$ and $NH_3 \cdot H_2O$ were *not* expected condensates in the solar nebula; how therefore could Titan's CH_4 be explained?

To help answer the latter query, Prinn and Fegley (1981*a*) proposed that the conditions in well-mixed subnebulae around the giant protoplanets (Pollack et al. 1976) provided precisely the chemical thermodynamic and chemical kinetic conditions necessary to make CH_4 and NH_3 (not CO and N_2) the dominant N and C gases in these subnebulae. They stated in the abstract of their paper that "satellites of the Jovian planets which accreted in sufficiently cool parts of their circumplanetary nebula are therefore predicted to retain large amounts of NH_3 and CH_4 in the form of clathrate/hydrates." More explicitly for Titan, they state "Titan is expected to have retained significant amounts of NH_3 (as $NH_3 \cdot H_2O$) and CH_4 (as $CH_4 \cdot 6H_2O$) and smaller amounts of HCN. If solar nebula temperatures at Saturn were equal to or even lower than 60 K, then retention of first N_2 (as $N_2 \cdot 6H_2O$) and then CO (as CO $\cdot 6H_2O$) is also possible." However an important cautionary statement was also made: namely mass-balance considerations indicated that complete condensation of CH_4 and NH_3 as $CH_4 \cdot 6H_2O$ and $NH_3 \cdot H_2O$ required more than *all* of the available water leaving *none* for forming the N_2 and CO clathrates. In addition, Lunine and Stevenson (1985*a*) give theoretical arguments and Davidson et al. (1987) give experimental results indicating CO clathrates are more stable than N_2 clathrates. Hence a model for the origin of Titan's atmosphere involving degassing of clathrates and hydrates would potentially yield copious amounts of NH_3 and CH_4 but clathration and subsequent degassing of CO and N_2 was problematical particularly for N_2.

Owen (1982*b*) later addressed the alternative possibility that Titan obtained its atmosphere by direct gravitational capture of N_2, CH_4 and other gases onto the primordial Titan. However, he ruled out this possibility due to the absence of the substantial amount of Ne (solar abundances of Ne and N are comparable) expected in a solar composition atmosphere after hydrogen loss. He reiterated the probable importance of methane clathrate suggested by Miller (1961), Lewis (1972*a*) and Prinn and Fegley (1981*a*) and also proposed specifically that the N_2 on Titan was derived from degassing of $N_2 \cdot 6H_2O$. From a cosmogonic viewpoint this is very difficult to justify. In particular, the high ice/rock ratio inferred for Titan from its density requires that much of the oxygen in the gaseous medium in which it formed be present as H_2O; this means that CO cannot be the major form of oxygen and hence $CO < CH_4$ as it is in the Prinn and Fegley (1981*a*) subnebula. However, the same chemical-dynamical conditions that yield $CO < CH_4$ also yield $N_2 < NH_3$ (see Figs. 2 and 3). As already noted, the formation of $N_2 \cdot 6H_2O$ in NH_3- and CH_4-rich subnebulae is improbable indeed and would need to be preceded by copious $CH_4 \cdot 6H_2O$, $NH_3 \cdot H_2O$ and $CO \cdot 6H_2O$ formation. These cosmogonic arguments point therefore to formation of Titan in a CH_4- and NH_3-rich subnebula

by a process of accretion of rock and $NH_3 \cdot H_2O$ hydrate and $CH_4 \cdot 6H_2O$ clathrate as proposed by Prinn and Fegley (1981*a*) with the N_2 atmosphere being a photochemical and/or shock-chemical byproduct of outgassed NH_3 (see chapter by Lunine et al. for a discussion of relevant photochemical and shock-chemical $NH_3 \rightarrow N_2$ scenarios).

The identification of $CH_4(s)$ and tentatively $N_2(l)$—and hence $N_2(g)$—on Triton would by analogy with Titan, suggest condensation in a CH_4-rich subnebula with the surface $N_2(l)$ again being a photochemical byproduct of $NH_3 \cdot H_2O$ solid and/or NH_3 gas photolysis. Without a firm number for the density of this satellite it is, however, premature to form any definitive conclusions. The same is true for Pluto and Charon as for Triton.

The most extensive data we have on ice-rich bodies is on their densities and geometric albedos. The low geometric albedos of many of the smaller satellites, together with solar light reflection spectra of some of these low-albedo satellites, suggests that these *dark* satellites may be rich in organic material (Cruickshank 1986). From a cosmogonic viewpoint this organic material could either be: (1) unprocessed interstellar material, or (2) Fischer-Tropsch-type organics formed from CO in the solar nebula, or (3) photochemical decomposition products of $CH_4 \cdot 6H_2O$ resulting from solar ultraviolet irradiation of the satellite surfaces after dissipation of nebula gases and sweepup of solar system dust. Thus, the presence of organics alone is not very definitive in answering questions about origin.

Interior models of ice-rich satellites can be constructed using feasible chemical compositions and fits to the observed satellite bulk densities. In principal, the ratio of silicates to volatile condensates deduced from such models can be used to infer certain chemical properties of the medium in which these satellites formed. In particular, the ratio of H_2O to silicates in ice-rich satellites depends sensitively on the [CO]/[total C] ratio in the medium (nebula, subnebula) in which the satellite condensed. If [CO]/[total C] $\simeq$ 1, then CO is the major oxygen reservoir followed by H_2O and then oxygen in anhydrous rocks (modeled here as SiO_2 + MgO + FeO to a first approximation); specifically [CO] : [H_2O] : [2Si + Mg + Fe − S] is 3.2 : 1.1 : 1.0 in solar composition. Alternatively, if [CO]/[total C] $\simeq$ 0 (i.e., CH_4 and/or organics are the major forms of carbon), then H_2O is the major oxygen reservoir and [CO] : [H_2O] : [2Si + Mg + Fe − S] is then 0.0: 4.3: 1.0 in solar composition. Thus there is 4.3/1.1 = 3.9 times more water available for forming pure ice in a CH_4-rich solar-composition medium than in a CO-rich medium.

For application to ice-rich satellites, it is convenient to translate the above number ratios into *ice* (H_2O solid; NH_3 hydrate or solid; CH_4, CO and N_2 clathrates or solids) to anhydrous *rock* (SiO_2, MgO, FeO, FeS) ratios. For satellites condensing in a CH_4- and NH_3-rich protoplanetary subnebula, we have (Prinn and Fegley 1981*a*; Fegley and Prinn 1986):

$$\begin{aligned}\text{ice:rock} &= 0.61 : 0.39\ (160\ \text{K} \leq T \leq 230\ \text{K}) \\ &= 0.64 : 0.36\ (95\ \text{K} \leq T \leq 160\ \text{K}) \\ &= 0.66 : 0.34\ (40\ \text{K} \leq T \leq 95\ \text{K}) \\ &= 0.74 : 0.26\ (T \leq 40\ \text{K})\end{aligned} \tag{46}$$

where the successive increases in ice mass fraction are due to successive formation of (i) H_2O (*s*), (ii) $NH_3 \cdot H_2O$ (*s*), (iii) $CH_4 \cdot 6H_2O$ (*s*) and (iv) CH_4 (*s*), respectively.

In constrast, for satellites condensing in a CO- and N_2-rich solar nebula, we have (Lewis and Prinn 1980; Fegley and Prinn 1986):

$$\begin{aligned}\text{ice:rock} &= 0.28 : 0.72\ (60\ \text{K} \leq T \leq 140\ \text{K}) \\ &= 0.35 : 0.65\ (20\ \text{K} \leq T \leq 60\ \text{K}) \\ &= 0.70 : 0.30\ (T \leq 20\ \text{K})\end{aligned} \tag{47}$$

where the successive increases in ice mass fraction are due to successive formation of: (i) H_2O(*s*), (ii) $CO \cdot 6H_2O$ and $N_2 \cdot 6H_2O$ and finally (iii) CO and N_2 solids.

Schubert et al. (1986) and Johnson et al. (1987) have discussed a range of feasible interior models for the ice-rich satellites of the outer planets. Johnson et al. (1987) computed specifically the following *system-average* ice : rock ratios (where "ice" is H_2O only):

$$\begin{aligned}&\text{ice:rock (Ganymede, Callisto)} = 0.44 : 0.56\ \text{(differentiated)} \\ &\text{ice:rock (Saturn satellites)} = 0.44 : 0.56\ \text{(mass average, i.e., Titan essentially)} \\ &= 0.61 : 0.39\ \text{(object average)} \\ &\text{ice:rock (Uranus satellites)} = 0.41 : 0.59\ \text{(differentiated)} \\ &= 0.50 : 0.50\ \text{(homogeneous)}\end{aligned} \tag{48}$$

For the Saturn system, Titan only was considered differentiated while for the Uranus system, Titania and Oberon only were considered as possibly differentiated. It is evident that the icy Galilean satellites and Uranus satellites have ice-to-rock ratios which lie between the values expected in CO-rich and CH_4-rich nebulae/subnebulae. The same is true for Titan but *not* for the other Saturnian satellites whose ice-to-rock ratio is essentially identical to that expected in a CH_4-rich subnebula.

If we accept the hypotheses that: (a) the regular satellites of the outer planets formed in subnebulae, and (b) the presence of CH_4 on Titan and Triton

means that CH_4 was present in appreciable amounts in these subnebulae, then ice-to-rock ratios which lie between the CO-rich and CH_4-rich nebula/subnebula ratios can be produced in at least three feasible ways:

1. Conversion of CO to CH_4 in the subnebula was incomplete (e.g., as may be possible in a poorly mixed subnebula);
2. Conversion of CO to CH_4 in the subnebula was complete but the subnebula (or the planetary disk system after the subnebula dissipated) subsequently accreted additional icy objects which formed in the CO-rich nebula;
3. Conversion of CO to CH_4 in the subnebula was complete but the larger ice-rich satellites lost some ice by blow off induced by post-accretional impacts as discussed in the chapter by Lunine et al.

Since all the outer planetary systems need to be augmented with elements heavier than H and He (by a process of accretion of solar nebula ice/rock solids without accretion of solar nebula gases), then methods (2) and (3) appear to us to be preferable at least in the absence of a quantitative demonstration of method (1). Note that based on our earlier discussion of Uranus, the ice-to-rock ratio in solar nebula objects will be increased (to lie between the CO-rich and CH_4-rich nebula values) to the extent that some of the solar nebula CO is converted to organics. Indeed, if it were not for the need to explain the regularity of the satellites and CH_4-rich satellites like Titan, the formation of the ice-rich satellites in a CO-plus organic-rich solar nebula (as opposed to a CH_4-rich subnebula) would appear quite feasible for explaining their observed ice-to-rock ratios (Johnson et al. 1987).

E. Comets

Prior to the Halley missions, the major parent volatile molecules inferred from both remote observations of cometary comae and analyses of stratospheric dust putatively of cometary origin were: (a) H_2O, (b) CO plus CO_2 with abundances $\approx$ 10 to 30% of H_2O, (c) HCN, NH_3, CH_3CN, etc. with abundances $\leq$ 1% of H_2O and (d) poorly characterized organic molecules $C_mH_nO_xN_y$ (which could serve as sources of coma C_2, C_3, CH, CN, etc.) with abundances perhaps a few % of H_2O (Delsemme 1982). Vega 1 analyses of the dust from Comet Halley indicated that the organic component of the dust consisted mainly of highly unsaturated compounds (Kissel and Krueger 1987).

Unfortunately this information on cometary volatiles by itself does not enable us to readily discriminate between two major possibilities: (a) interstellar material (dust, condensible gases) and (b) solar nebula condensates, as the parent material for comets. This is because the H_2O, CO clathrate, CO_2, NH_4COONH_2 (this contains a C $-$ N bond), NH_4HCO_3, HCN, and Fischer-Tropsch organics predicted in nebular condensates (Sec. III.B; also Lewis and Prinn 1980) bear too many similarities to the composition of (con-

densed or readily condensible) interstellar material inferred from astronomical observations, (CO, H_2O ice, HCN, carbonaceous compounds, etc; see the chapter by Irvine and Knacke). Nitrogen clathrate ($N_2 \cdot 6H_2O$) is predicted as a major low-temperature solar nebula condensate (Lewis and Prinn 1980) but the absence of N_2 in comets is plausibly explained by a greater stability of $CO \cdot 6H_2O$ over $N_2 \cdot 6H_2O$. Predicted kinetic difficulties in forming clathrates at low pressures (Lunine and Stevenson 1985*a*) are common to both the solar nebula and interstellar hypotheses for origin of cometary CO.

Early results from the Giotto Comet Halley mission provide what may prove to be definitive information on the (chemical) origin of Halley. The Giotto ion mass spectrometer data suggest production rates of CO and N_2 to be about 0.05 to 0.2 and < 0.01 to 0.1, respectively of H_2O production (Eberhardt et al. 1986; Balsiger et al. 1986); a result similar to that seen for previous (remotely-observed) comets. However, production rates of NH_3 and CH_4 are inferred from the same Giotto experiment tentatively to be as large as 0.01 to 0.02 and 0.02, respectively, of the H_2O production rates (Allen et al. 1987) implying $CH_4/CO \approx 0.1$ to 0.4 and $NH_3/N_2 > 0.1$ to 2. Both of these latter ratios are much greater than those seen in the interstellar medium and, if correct, argue strongly against accretion of Halley from pristine interstellar material (Allen et al. 1987).

Values of $NH_3/N_2 >> 1$ are however predicted in solar nebula solids (due to low-temperature condensation of NH_4HCO_3 and NH_4COONH_2) provided temperatures are not so low that N_2 clathrate or N_2 condense (see Table IV). A CO/H_2O ratio ≈ 0.15 is also predicted in solar nebula solids provided temperatures are low enough (and the pressure high enough) so that CO clathrate forms. Complete condensation of the solar abundance of C as CO clathrate would also use up all of the readily accessible cavities in the ice structure and thus inhibit N_2 clathrate formation. However, a CH_4/CO ratio as large as 0.1 in the solar nebula would require quenching of the $CO \rightarrow CH_4$ reaction in the solar nebula at temperatures as low as 700 K compared to a predicted quench temperature $\sim$ 1470 K and predicted CH_4/CO ratio $< 10^{-7}$ (see Fig. 2). Also the Halley NH_3/H_2O ratio of 0.01 to 0.02 significantly exceeds the *maximum* predicted NH_3/H_2O ratio in the solar nebula of 0.002 (the latter maximum ratio corresponds to the minimum quench temperature for $N_2 \rightarrow NH_3$ being 480 K due to total oxidation of Fe catalyst at lower temperatures). Therefore Halley does not appear to be a pristine solar nebula condensate either.

We have emphasized earlier that the thermodynamic and kinetic conditions necessary to produce CH_4 and NH_3 from CO and N_2 would occur in well-mixed subnebulae of the giant planets but not in the solar nebula (and not of course in the even cooler and less dense interstellar clouds). Table IV shows, however, that the CH_4/CO and NH_3/N_2 ratios in pristine subnebulae condensates are much greater than seen in Halley. An obvious working hypothesis to explain Halley is in fact a *heterogeneous mixture* of a small amount

(e.g., 10%) of CH_4-rich subnebula condensate with a large amount (e.g. 90%) of CO-rich condensate of solar nebula or interstellar cloud origin.

We have two suggestions for producing such mixtures which are in fact analogous to our suggestions (1) and (2) for explaining the ice/rock ratios in ice-rich satellites. Let us first suppose that the giant planets possessed well-mixed subnebulae (accretion disk or spin off or impact generated). After the nebula and subnebulae gases are significantly dissipated, we are left in the outer solar system with CH_4-rich (subnebula-derived) objects orbiting around the giant planets and CO-rich (nebula-derived) objects orbiting around the Sun. Clearly some CO-rich solar system objects are expected to sweep through the giant planetary ring systems and accrete CH_4-rich material and *vice versa*. Alternatively, we can suppose that one or more of the giant planets possessed partially mixed subnebulae in which condensation of objects with small amounts of CH_4 (mixed outward from the inner disk) and large amounts of CO (mixed inward from the solar nebula) were a natural occurrence (since we must also explain CH_4-rich objects like Titan or Triton and since an impact-generated disk is likely for Uranus, it is unclear what the candidate giant planet is in this scenario). The dynamics of both suggestions need to be investigated to establish their viability and relative probability.

Nevertheless, the observation of such large amounts of CH_4 and NH_3 in Halley is persuasive evidence that at least some of the material in *this* comet (but not in CH_4-poor comets) is neither of solar nebula nor interstellar origin but is material condensed in a subnebula of one of the giant planets.

V. CONCLUSIONS

In this Chapter we have attempted to synthesize for the first time the wide variety of observational data and theories pertaining to the origin of the most volatile elements (C, N, H, O) in the solar system. It is clear that this subject is in an exploratory stage and seemingly *firm* conclusions may subsequently prove to be illusions. With this caveat in mind we offer the following as *firm conclusions:*

1. The starting materials were gases and grains in interstellar cloud(s).
2. As the nebula evolved, these gases and grains were at least partially reprocessed chemically; in particular the nebula was extensively physically mixed and chemically reprocessed (but not necessarily chemically and isotopically homogenized) at least out to 4 AU.
3. The major type of chemistry in the nebula was thermochemistry driven by the thermal energy of the nebula itself. Chemistry in lightning discharges and photochemistry driven by stellar photons were secondary but with their relative importance increasing with increasing radial distance. Solar photons played very little role if any because they were absorbed in the

very hot thermochemically controlled innermost nebula. Radiochemistry driven by ^{26}Al was minimal.

4. The gas-rich solar nebula and the dust-rich early post-solar nebula disk were highly opaque to ultraviolet radiation limiting severely the influence of the enhanced ultraviolet flux from the young Sun in the early solar system.
5. The reduction of N_2 and CO to NH_3 and CH_4 was kinetically inhibited in the solar nebula but not in the subnebulae of giant planets. Thus the nebula was (like interstellar material) rich in N_2 and CO (and organics formed from it) while subnebulae were rich in CH_4 and NH_3.
6. Vapor-phase hydration of silicates, like the chemical reduction of N_2 and CO, was very probably kinetically inhibited in the solar nebula.
7. The regular satellites of the outer planets originated in well-mixed subnebulae of these giant planets created by the accretion process, by spin off or by a massive impact.
8. Certain volatile ratios (e.g., CO/CH_4, N_2/NH_3, H_2O ice/silicate) in ice-rich bodies are diagnostic of their origin. For example, the CH_4 on Titan and Triton argues for their formation in a CH_4- and NH_3-rich giant-planetary subnebula while the observation of CH_4 and NH_3 (as well as the more-abundant CO and N_2) in Halley implies that at least some (see Conclusion 9 following) of the material in this comet is neither of solar nebula nor interstellar origin but was condensed also in a giant-planetary subnebula.
9. After the dissipation of the nebula, collisions between ice-rich solar system objects formed in the nebula and giant planetary satellite objects formed in subnebulae are inevitable and could produce hybrid objects characterized by a heterogeneous mixture of CO-, N_2-, CH_4-, and NH_3-containing ices.

How can our understanding of nebular chemistry and the origin of solar system volatiles be improved? Although we make no attempt at a comprehensive answer to this question, we think the following points worth emphasizing:

a. Current models of the solar nebula and protoplanetary subnebulae have recognizable important shortcomings. For example:
   (i) models of chemical processes are hampered severely by a lack of quantitative laboratory studies of the kinetics and mechanisms of a wide range of important gas/gas and gas/solid reactions (e.g., Fischer-Tropsch-type reactions) under conditions relevant to the nebula and subnebulae;
   (ii) current dynamical models ignore the quadratically nonlinear nature of momentum transport thus precluding expected counter-gradient momentum fluxes and leading to the erroneous conclusion that trace constituents in the nebula and subnebula must have been poorly mixed.

b. Current observations of many volatile-rich bodies in the solar system are insufficient to constrain meaningfully our knowledge of the chemistry of the solar nebula. We emphasize in particular the need to sample and analyze unperturbed material from comets, asteroids and ice-rich satellites and not to rely just on inferences from remote sensing and analyses of the (perturbed) material in cometary emanations.
c. Through improved observations, our knowledge of other protostellar systems needs to be expanded substantially so that it can provide definitive insights and constraints on the origin of the solar system.

If the need for these and other improvements is not already self-evident, it is worth closing by noting that, based on our current knowledge of solar nebula chemistry, we still do not know definitively in what form carbon, nitrogen and water were incorporated into the inner planets or how much interstellar material survives in the solar system today and where it is. We hope that one day such questions will have definitive answers.

Acknowledgments. We thank M. Allen and T. Johnson for discussions and manuscripts provided prior to publication, B. Vanderlaan for assisting with coding while working in the MIT UROP Program, G. Rodriguez for $T_EX$nique, and D. Souza for drafting. We also thank D. Stevenson and Y. Yung for their reviews of the original manuscript. Some of our stronger and clearer statements were made in response to their comments. This research was supported by grants from the National Science Foundation (Atmospheric Chemistry Program) and the National Aeronautics and Space Administration (Planetary Geochemistry and Materials Program, Planetary Astronomy and Atmospheres Program, and Innovative Research Program).